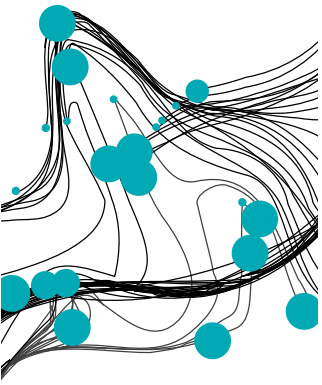

RAM ROBOTICS AND MECHATRONICS

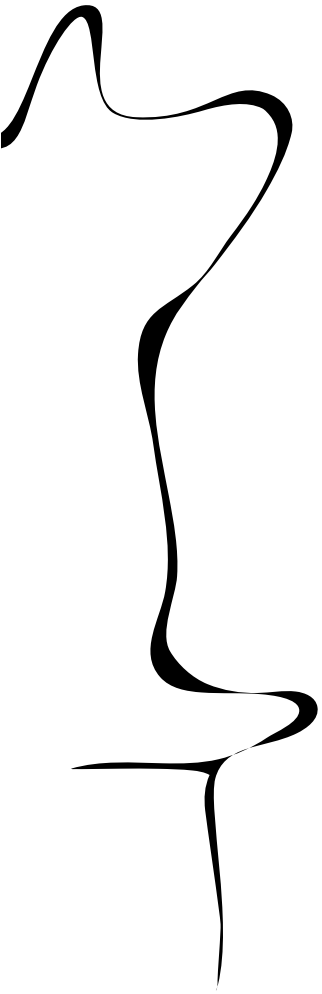

IMPACT OF DISPLAY TECHNOLOGY ON HEPATIC PERCUTANEOUS TELEOPERATION PROCEDURES WITH HAPTIC FEEDBACK

N.H.A. (Nick) van Lange

MSC ASSIGNMENT

Committee:
dr. ir. M. Abayazid
M.S. Selim, MSc
dr. ing. G. Englebienne

August, 2024

052RaM2024
Robotics and Mechatronics
EEMCS
University of Twente
P.O. Box 217
7500 AE Enschede
The Netherlands

UNIVERSITY OF TWENTE. | TECHMED CENTRE
UNIVERSITY OF TWENTE. | DIGITAL SOCIETY INSTITUTE

Contents

1 Introduction

1.1 Abstract

This thesis investigates the impact of display technology on hepatic percutaneous teleoperation procedures with force haptic feedback. The research includes the implementation of a teleoperation setup specifically designed for teleoperated hepatic percutaneous insertions through use of a robotic arm. In addition to featuring a novel haptic feedback system that utilizes viscosity control and separation of forward and lateral control. Additionally, a comprehensive visualization environment was developed for both an augmented reality head mounted display(AR HMD) and autostereoscopic 3D. To evaluate the effectiveness of these display technologies, a comparative study was conducted with participants to determine the effects. Results indicate that 3D displays significantly reduced procedure time, while maintaining accuracy comparable to standard 2D monitors. Although AR HMDs also accelerated task completion, usability was compromised. Users showed a clear preference towards the use of a 3D display.

1.2 Context

Minimally invasive surgery is an important part in liver cancer treatment. One of the initial steps is to perform a liver biopsy, to determine possible malignant presences. Further treatment can be done in the form of ablation therapy, in which the malignant tissue is destroyed using a needle that emits high frequency radio waves. Both of these treatments use a needle insertion procedure [1]. Over the last twenty years, several technological advances providing assistance to the liver surgeon for visualizing intraoperative navigation have been developed [2]. Augmented reality (AR) is the concept of projecting a digital object on real-life scenes. It has the potential to provide surgeons with essential information to optimize navigation in complex surgeries to reduce intra- and postoperative complications [3]. In intraoperative procedures it can assist in showing the position of organs, veins and bone to the surgeon, by projecting them on top of the body. For example, a complete system is already in the market for spinal surgery [4]. AR in liver surgeries is often investigated, according to Acidi et al.[2]. AR is being put into effect in open surgeries as shown by Fida et al.[5]. AR can reduce the risk of an operation by giving the surgeon improved sensory perception [6]. The most important AR functionalities for this research area include visualization, path planning, and surgical navigation [7]. There are still concerns about the movement of the internal organs during surgery, which can affect the exact positioning of the AR environment. Other challenges in the medical field regarding AR are: legal issues, affordability, technical limitations, latency, safety problems and a lack of robust infrastructure to support the AR systems [8][9].

Haptic feedback is the concept of giving feedback in the touch related sense. This can be through either kinesthetic or tactile feedback. Tactile feedback relates to sensations felt on the skin's surface, for instance, feeling the texture of a wooden surface. Kinesthetic feedback is feedback related to body movement and position. An example of kinesthetic feedback is feeling a feedback force in response to moving a joystick. For needle insertion, haptic feedback can aid in accurate needle alignment.

There are different use cases for telesurgery, it can be used with a specialist to operate from a distance, increasing the availability of experts. Certain types of procedures are available in limited hospitals. A comprehensive telesurgery network could improve patient outcomes by reducing travel time and associated burdens. The COVID-19 pandemic underscored the critical role of telesurgery in mitigating infection risks, as surgeons can operate remotely on patients with infectious diseases [9]. An additional use case is reducing the amount of radiation

surgeons receive by CT-guided surgeries, the surgeon is able to perform the surgery outside the CT-room.

Telesurgery can be combined with AR and haptic feedback in needle insertion surgeries. Little research has been found with the combination of AR and haptic feedback in remote needle insertion surgeries. Research has explored combining AR with haptic feedback for training purposes [10]. Combination between AR and haptic feedback in telesurgery has been explored in Fu et al. [11] where it was used for teleoperated ultrasounds. Teleoperated needle insertion surgeries combining AR and haptic feedback are largely unexplored. In this research, a comparison is made between an AR head mounted display(HMD), a 3D display and a regular screen in their value for visual information transfer in remote needle insertions.

1.3 Objective

The main objective of this paper is to study the effects of different visualization techniques in teleoperated robotic hepatic percutaneous procedures. AR HMD, a 3D display and a 2D screen are compared. These are integrated with a force haptic feedback system. To achieve this, a system is built that combines AR and haptic feedback in a telesurgery system capable of liver tumor needle insertions. The system should be capable of accurately updating the augmented reality environment in real time. A needle should be controlled at a distance using the haptic feedback controller, and the augmented reality environment should provide a clear visualization of the scene at a distance.

1.4 Research Setup (Research Questions)

Following the main objective of improving teleoperated minimally invasive surgeries through AR, this led to the main research question:

> How can augmented reality improve haptic feedback controlled remote surgery for hepatic percutaneous procedures?

This question directly relates to the objective of improving remote controlled surgeries through visualization with AR. AR offers the potential to provide surgeons with significantly richer visual information about the remote scene compared to traditional methods. Investigating the aspects in which visualization can be improved leads to the following sub-questions:

> What are the requirements for an AR system in haptic feedback controlled remote surgery for hepatic percutaneous procedures, and how to validate these?

What is required of our system to be able (at least in theory) to achieve a successful, reliable remote operation. Many of these requirements can be found in literature. Some of these requirements provide indicators that have to be measured during the testing. The measurements provide evidence for the validation of the system. Other requirement are necessary for the system to be useable in the first place.

> What visual information is important to convey in remote surgery for hepatic percutaneous procedures?

An important aspect will be the visual information that is shown and how it is shown. There are many different approaches to showing visual information. It is vital to find out what the most important information is to convey at each moment. Examples of information that can be visualized is the needle pose, position of the liver and liver tumor and the exact position of the incision point. More general information about the condition of the patient could also be

implemented. In part, this question can be answered empirically during the building of the system. By testing with different persons, to observe the different effects. Some frameworks will be taken from literature as a starting point. Different display techniques can be used to display this visual information, which leads to the next question.

> How do different display techniques(AR HMD, 3D Display) compare in meeting the requirements?

There are multiple ways of providing the visual information of the remote scene. Even within AR, there are different devices which can be used. One such example is an AR HMD, which provides an augmented reality view of the surroundings through glasses. Another is using an autostereoscopic 3D display. There was research done comparing the effects of display techniques for needle insertions[12], but never for remote surgery.

1.5 Scope

The focus is specifically on liver tumor ablations and biopsies. Other surgical procedures are considered to be out of scope for this research. Only needle insertions are considered, the needle retraction is not taken into consideration. Another aspect is the visual aids that will be used in the AR environment. The main focus is on the display techniques, haptic feedback is used but is not the primary interest. The display techniques are limited to a baseline of a 2D display, a 3D display and an AR HMD. Different visualization apparatus are compared. While haptic feedback is an integral component of the system, its configuration and parameters will be fixed to minimize variables.

2 Background

2.1 Augmented Reality

The term augmented reality first appears in the 1990's. It was coined by two researchers at Boeing, who introduced it in an article [13]. Currently, there are many use cases and applications for augmented reality. It is used in fields such as, advertising, military applications, medicine, gaming, forensics and navigation [6]. Augmented reality encompasses a multitude of systems, including monitor-based systems that overlay virtual objects onto live video feeds of the real world. Head mounted displays (HMDs) provide a more immersive experience. They come in two forms. The first is optical see-through. Which is commonly implemented using an optical beam splitter. The light of the environment is mixed with projected light from the head mounted display, given the appearance as if the virtual object is on top of the environment. The other variant uses video see-through. As the name implies, the real environment is filmed using a camera attached to the HMD. This footage is played in the glasses and virtual objects are projected on top of the footage. Finally, there are projection based methods. In these projection based methods, images are projected on top of objects using projection based systems, such as a projector.

AR is characterized by the integration of real and virtual world, it is different from Virtual Reality(VR) and Mixed Reality(MR). In Figure 2.1 the difference between the terms is shown. In VR, the user is in a fully digital world, without any real-world elements. Mixed reality is the blurred line between VR and AR. Virtual element are able to interact with the real-world, or vice versa.

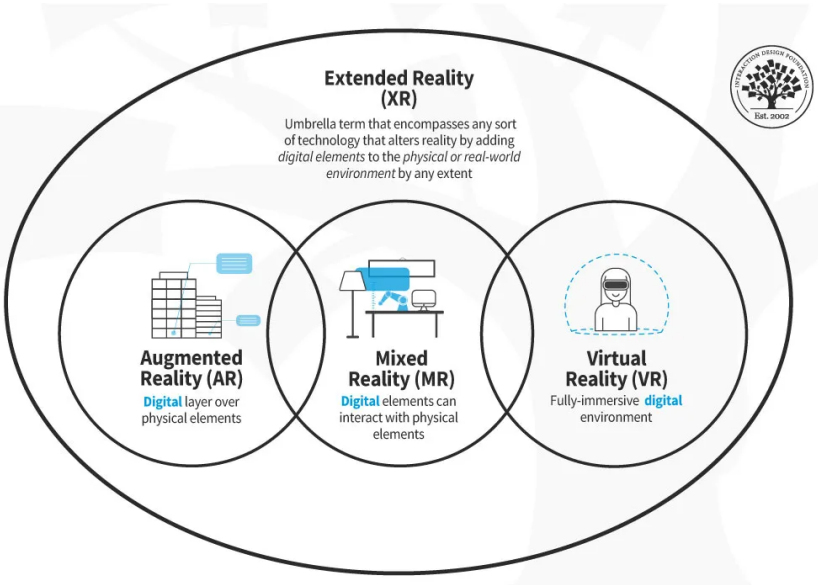

Figure 2.1: Differences between augmented reality and virtual reality [14]

2.2 Augmented Reality in Medicine

AR and VR are upcoming in medicine with increasing interest from researchers. In Figure 2.2, the number of citations and publications each year can be seen. There is a notable increased interest over time. Research has been done for use-cases such as surgical training, rehabilitation and surgical assistance. The most common use case is surgical simulation for the purpose of training new surgeons [15].

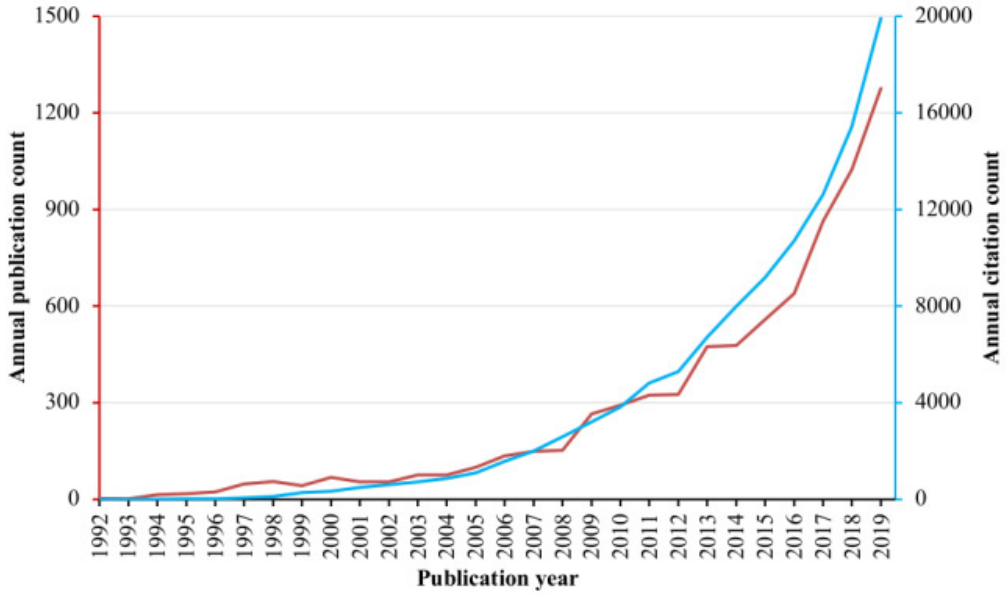

Figure 2.2: Virtual reality related research in medicine, annual citations and publications [15]

For liver tumor ablation surgery, Endosight is a system capable of projecting the internal organs on top of the skin of the patient [16]. The system was clinically tested on eight patients with successful procedures in all operations. They achieved a high targeting accuracy of 3.4 mm ± 0.7 mm, with the largest offset distance 4.5 mm. In Figure 2.3 the AR projection can be seen. The liver, rib cage and the liver blood vessels are modeled and shown on top of the patient. 3D models are created based on CT scans. Using markers on the skin of the patient, the AR system can register where the models should be placed. Furthermore, a surgical path is shown from the needle tip to the target destination.

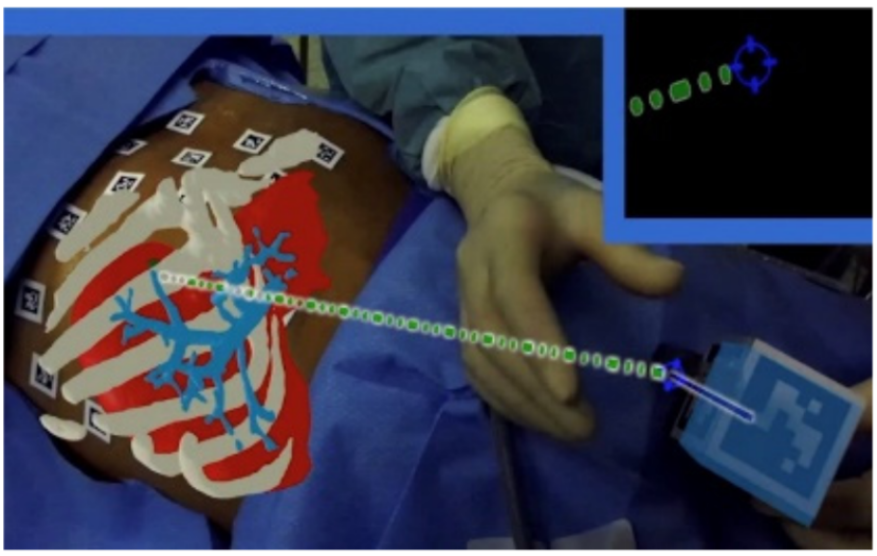

Figure 2.3: Visualization of the Endosight system in a clinical trial[16].

2.3 Autostereoscopic 3D

A common view in many movie theaters is the use of 3D screens. A popular phenomenon slowly faded away. These displays worked in combination with polarized glasses to create the

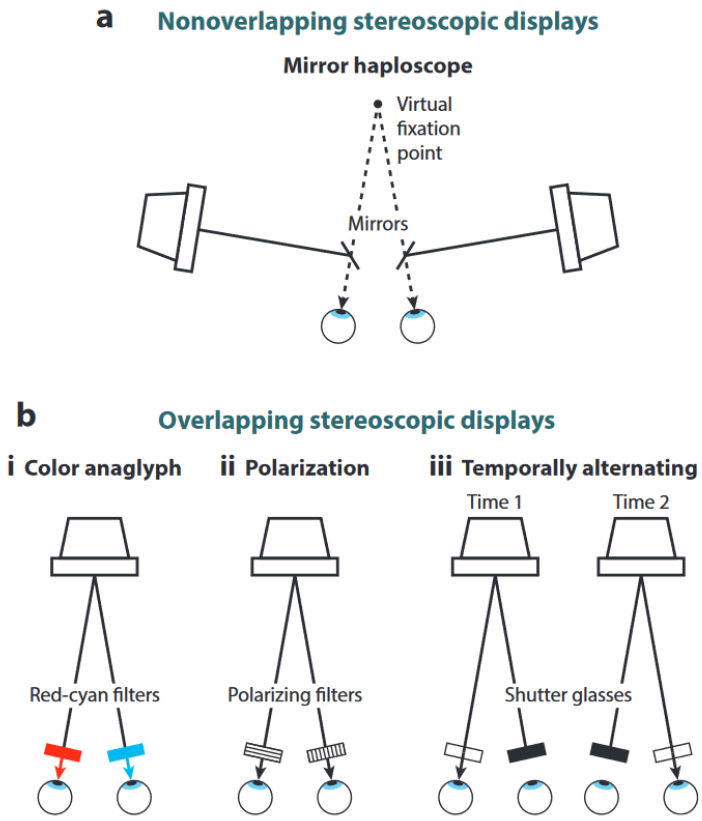

Figure 2.4: Different types of stereoscopic displays [17].

illusion of 3-dimensional images. The general idea is that the left eye and right eye see different images, tailor-made for each viewpoint. this creates a 3D image in the mind by recreating the parallax effect. multiple methods of creating overlapping displays were devised. In Figure 2.4 different methods can be seen. Anaglyph 3D by using chromatic opposite color filters, usually red and cyan. Depth information is encoded in the color and by wearing glasses with these filters the image is combined into a 3D image. A similar is concept is devised with polarized 3D, in which images are encoded in vertical and horizontal wavelengths. Each eye has a different oriented filter and receives the according images. The final overlapping stereoscopic technique is by temporal alternation, where the user wears stutter glasses in phase with the display.

For realizing autostereoscopic 3D, multiple methods have been devised with varying success. The two main methods involve estimating the position of the eyes and delivering split images from the screen. One method is to use a parallax barrier with precisely aligned slits or barriers in front of the LCD screen, that deliver the two slightly different images to each eye. The technique can be seen in Figure 2.5. This was the system implemented on the Nintendo 3Ds to achieve the 3D effect [18]. The other method is to use a lenticular display. This method is similar to the parallax barrier, but instead uses cylindrical lenses arranged in parallel on a sheet. The cylindrical lenses refract light from the interlaced images in a way that each eye receives a different image. A big disadvantage for these methods is that they only work for a singular person, since the functioning depends on the position of the eyes. There are proposals to enable multiple viewpoints, but these come with major downsides, such as resolution degradation [18].

3D vision can give a surgeon critical depth and spatial information at a glance. Not only is depth embedded in the rendering of the scene, estimation of depth can further be achieved by a

simple tilt of the head due to motion parallax. Motion parallax is one of the major contributing factors in depth perception, increasing the potential informational transfer to the user [19].

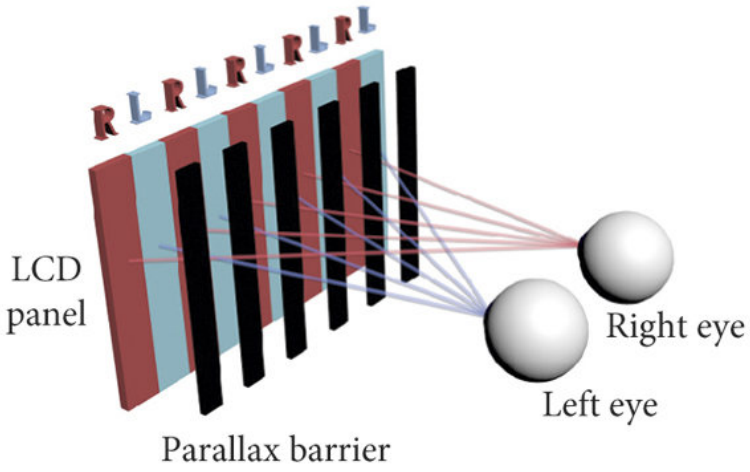

Figure 2.5: The effect of a parallax barrier [20].

2.4 Telesurgery and Robotic Surgery

Telesurgery is the concept of performing surgery remotely. A surgeon controls a robotic surgery setup from a different location. The first remote surgery ever performed was on a patient from France in 2001. It was remotely controlled by surgeons in New York [21]. This shows the feasibility of telesurgery. Potential benefits of telesurgery include reaching remote areas with the best surgeons. A highly qualified surgeon would be able to service a remote range of areas from a single location. It could give options for surgeons working at different medical centers to cooperate on the same surgery [22].

Disadvantages that prevent telesurgery from entering the market are cost, lack of surgeons trained in teleoperation, connectivity issues and legal issues.

Robots are already used in laparoscopies, with multiple robots on the markets. The most prominent of these robots is the Da Vinci surgical system [23].

2.5 Haptic Feedback

The direct definition of haptic is that it is related to a sense of touch. Haptic sensations can be broken down into two main groups, tactile and kinesthetic. Tactile feedback regards to feelings on the skin, such as the texture of an object or feeling a vibration. An example of a commonly used tactile feedback system is the vibration motor inside smartphones. A subtle vibration upon keypress provides instant confirmation that the input has been registered, improving typing accuracy and speed. Kinesthetic related to more positional attributes, such as feeling the needed the force to open a door. An example of a kinesthetic haptic device is an advanced flight simulator. These advanced simulators replicate movements made by the virtual plane, resulting in feedback through motion.

In Weber et al. [24] the benefits of force feedback in medicine is shown. Showing major improvements in general task performance and minor improvements in task completion time. Providing force feedback is essential during teleoperation or VR simulations to keep a high performance level. This enables the user to feel a simulated force based on what the actuated object would feel. Furthermore, constantly updated haptic information can aid understanding the positions of objects in space. It can also potentially ease the handling of a controller by giving forces that stimulate desired movement. For example, it can stop a user from making high

frequency movement by making the controller hard to move, encouraging the user to make low frequency smooth movements. It can work in combination with visual information, decreasing the cognitive load in the face of excessive information.

2.6 Hepatic Percutaneous Procedures

Hepatic percutaneous procedures encompass a range of minimally invasive interventions performed on the liver via puncture through the skin. These procedures have gained significant prominence in recent years due to their less invasive nature, reduced postoperative complications, and improved patient outcomes compared to open surgical approaches [25].

Hepatic percutaneous biopsy is a procedure performed to obtain a small sample of liver tissue for examination. This procedure is crucial for establishing a diagnosis of liver diseases. The procedure is commonly aided by ultrasound, computed tomography (CT), or magnetic resonance imaging (MRI) guidance to ensure accurate needle placement.

Hepatic percutaneous ablation is an intervention aimed at destroying malignant liver tissue, primarily liver tumors. Various energy sources can be employed for ablation, with the main choice being radio frequency ablation [26].

Both procedures follow similar steps:

- Before inserting the needle, the entry point, a safe path, and the final needle position are carefully planned by reviewing pre-procedural imaging.
- Insertion of a specialized needle through the skin and into the target liver lesion. Under Image-guided supervision.
- Performance of the ablation or biopsy procedure [26].

3 Design

3.1 Requirements

Some of the requirements are for a theoretical complete system. This will be out of scope for the testing in this project. These requirements will be marked by a * meaning they are treated as out of scope and won't be validated.

3.1.1 Functional Requirements

- The system needs to be able to perform needle insertion procedure.
- The AR environment should include a moving needle and a 3D model of the liver with a tumor.
- The needle should be controlled using a force haptic feedback controller.
- The system should support remote surgery visualization and needle control for telesurgery on the liver phantom.
- The virtual needle should move in accordance with the actual needle in the robot, tracking its position and extension.
- The environment should provide a strong sense of depth perception for both the liver and needle.

The system needs to be able to perform the surgery. The virtual environment requires 3 models to visualize the procedure. At a minimum, a virtual needle, liver, and tumor are required. These virtual models should be realistic and based on real scans to enhance authenticity. To test our objective of using haptic feedback for control in the telesurgery the needle should be controlled by a haptic feedback device. The complete system will have to work with a phantom setup, so that actual results can be measured from the test surgeries. Furthermore, the needle in the robot should be controlled with the haptic feedback, the virtual needle should show the movement of the real needle. This means the virtual needle should mimic the movement of the actual needle in speed, position and rotation. One of the main issues that plagues remote surgery is a lack of depth perception on a 2D screen [27], the AR environment should resolve that problem so that it gives depth perception for the needle and the liver. This may be achieved by having depth perception the traditional way, e.g. having two eyes. Another addition can be visual cues that help, such as a bar that shows how far you are from the incision point.

3.1.2 User Requirements

- The AR environment should offer an intuitive user interface for users.
- The system should be usable by non-technical experts, making it accessible to medical staff.*
- Users should be able to use the system comfortably, with no discomfort or motion sickness.

An intuitive user interface helps with acclamation to using the system, as shown in [28]. A future telesurgery system will be in hospitals and used by medical staff. Medical staff in general do not have high technical training. The system should therefore be able to be used by non-technical experts in all steps. Surgeons might have to use the system for extended periods of time, if the system causes discomfort or motion sickness the system would be unusable. This can be measured by the usability of the system.

3.1.3 System Integration Requirements

- The AR environment should be capable of displaying data from a measurement system through the Robot Operating System (ROS).

- The operating process should be straightforward and manageable by non-experts within a hospital setting.
- The visual environment should support network communication to control the robot arm setup and receive feedback using ROS

ROS is commonly used in robotic systems, for integration it is good if all separate parts of the system can communicate through ROS. Again the system will be used by medical staff which are non-technical staff, so they have to be able to set it up. The telesurgery system could be at a distant location, communication on such long distances is best done over the internet. Therefore, the system should use network communication between the robot arm setup and the user side.

3.1.4 Performance Requirements

- The system's latency should be low.
- The system should operate in real-time, providing immediate feedback.
- The setup time should not be too long.*
- The system should not experience lag or performance issues due to graphical demands.
- Visual overload and cluttering should be kept in check
- The system should exhibit robust performance, with high reliability and stability.*

As determined in Xu et al. [29] telesurgery systems have great performance with latency below 200ms. Nearing 400 ms they are still useable, but longer delays are unusable. Telesurgery is done in real-time, so the system should be real-time. If setup time of the system is too long, it is not worth using. Lag and low performance can provide unpleasant working environments, systematic lag due to graphical demands should be lowered by reducing quality of the graphics if necessary. Minimizing visual overload is necessary to prevent subjects from feeling overwhelmed. Furthermore, it can cause distractions and eye strain. The system should also not be used in unstable networks, the system should detect when performance is low to ensure that it will only proceed when the environment is stable.

3.2 Materials

For the development of the system, several materials are chosen and combined. Each of these tools has its role in the complete system, and fulfills some part of the requirements. Such as actuating the needle or providing a framework for building the software application. Below, the specific tools and technologies are discussed.

3.2.1 Magic Leap 2

AR technology has come a long way in recent years. With more devices reaching the market. Magic leap 2 is one such recent model that has been released. In Figure 3.1 it can be seen. One relevant advantage of this model over other AR models is the high FOV (field of view) of 44.6 x 53.6 x 70°. It also boosts a high resolution of 1440x1760 per-eye. In these aspects, the Magic Leap scores the best of all released AR devices, at time of writing [30]. In previous research of Heinrich et al.[12] identified resolution and FOV as major limitations in usability. The Magic Leap 2 addresses these issues effectively. Additionally, the Magic Leap 2 contains its own compute pack, this makes it functioning independent of other hardware.

3.2.2 Unity

Unity is an engine made for game development. It is commonly used for making higher level AR applications. Unity uses C# for its programming language. In Fu et al.[11] it was used for the development of an AR environment for use in a remote ultrasound operation. For this system, it proved to be a good tool to use since it provides a framework for our AR application.

Figure 3.1: The Magic Leap 2 AR HMD

Unity was chosen over other options because it is the recommended platform for the Magic Leap 2 and aligns with prior experience. Additionally, Unity has support for the 3D display application in the form of the Leia SDK. Finally, the made application can be used for our 2D application, by turning off the 3D rendering.

There is support for ROS in libraries, such that can be used to connect it to ROS, which can be used to connect it with the other parts of the system. The used library is the ROS TCP connector library, provided by Unity Technologies themselves. Unity will handle all the visual elements that will be used. For example, it will handle the helpful visual elements that will aid the surgeon. It will render the surgical path vector, needle and show the incision point. Unity will render our models, such as the phantom, liver and needle. Furthermore, camera controls and UI are implemented.

Figure 3.2: The Franka Research 3

3.2.3 Franka research 3

The needle has to be actuated to perform the needle insertion. In an ongoing research at RAM, the movement of the liver is tracked during surgery. In this setup, a needle insertion surgery is performed on a phantom liver. This same robot setup can be utilized for this project to simulate the "real" world part of the environment. This setup uses the Franka Research 3 robotic system [31]. An image of this robotic arm can be seen in Figure 3.2. The robot arm holds the needle and works as a slave device for the master haptic feedback device. The robot arm is capable of performing the full range of motion required during the surgery. In Gromniak et al. [32] the

same robot arm is used for post-mortem biopsies. This robotic system is controlled with ROS from a computer which runs on Linux.

3.2.4 Omega 6

The Omega 6, a six-degree-of-freedom force feedback device manufactured by Force Dimension, is employed for this research. This device is able to fulfil the role of a force feedback device. It serves as the input device for the needle movement control. The device only has force feedback in the translational directions, it lacks rotational feedback. The haptic device has a workspace of 160 x 110 mm. It can give a maximum translation force of 12 N. The effects of rotational feedback are something that should be looked after in further research. The device can be seen in Figure 3.3. It helps that the controller is vaguely needle shaped, this makes it more intuitive for the desired use. The effectors also contains a button, which can be incorporated in a control scheme. The device enables users to control the needle. In Aggravi et al. [33] they use the same device for a haptic needle teleoperation setup, validating its suitability for this application

Figure 3.3: The Omega 6 Haptic feedback device with 6 DOF movement and 3 DOF force feedback.

3.2.5 ROS

All the separate systems have to be able to communicate with each other. Robot Operating System (ROS) is a set of software frameworks designed for developing robotic software. It delivers libraries for common applications in robotic systems.[34] Furthermore, it can handle communication between a plethora of different software systems, no matter the programming language. For our case it will be used to connect the unity environment with the haptic feedback device, the needle insertion machine and any other necessary sensors. ROS is chosen over ROS2 because the Franka setup at RAM is only supported by ROS.

3.2.6 Barco 3D display

Barco is a technology company that specializes in designing and developing innovative visualization solutions. Barco's primary areas of expertise include: visualization and healthcare solutions. They allowed us to borrow a prototype for this research. The display provides us with the means for the other two modalities. The screen works through a combination of an integrated depth camera and lenticular display. The camera tracks the user's eye location and accordingly renders specific images for each eye, as illustrated in Figure 3.4. This provides the user with a 3D effect. As an extra benefit of this method, motion parallax can be implemented based on movement of the head. A disadvantage of this method is that it only works for one person, for other viewers the display has an overlapping effect, which is not pleasant to look at. The same display is used for the 2D modality.

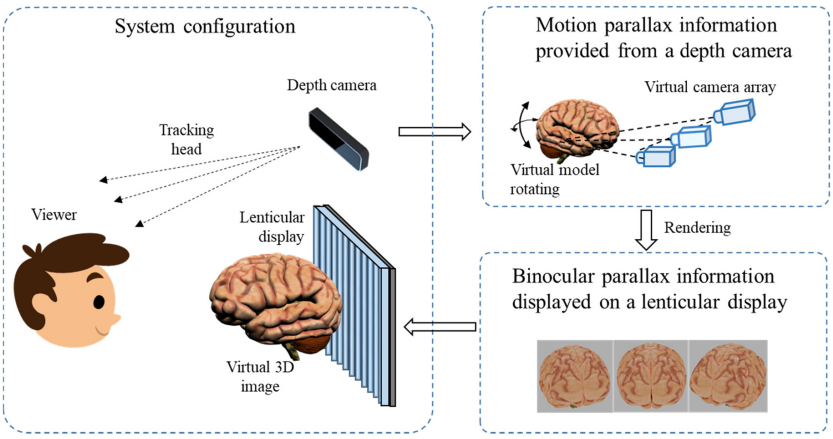

Figure 3.4: The methodology used by the Barco display[35]

3.2.7 Phantom

In medical simulation, there is a need for tissues with similar mechanics as skin and organs. Needle insertions are not different. there is a need to mimic the tissue which the needle penetrates. According to Armstrong et al. [36] the most suitable materials for needle insertions are PVA, PVC and silicone. The materials and factors can be seen in Table 3.1. PVA hast the most realistic dynamics for needle insertion, but comes at a price of low durability and difficult storage methods. Hydration based material have to be stored in a solution of water and an antimicrobial agent to prevent bacterial and fungal growth [36]. PVC is a little less realistic but a lot more durable. PVC was selected as the material for the phantom instead of PVA. PVC is more durable than PVA, making it suitable for long-term use, avoiding the challenging storage demands of PVA.

The volume and depth of the phantom has to be large enough that realistic depths and angles of insertion can be simulated. In Long et al. [37] operating depths are observed to be in the 71.7 ± 16.7 mm range. To simulate similar operating depths, the phantom's height is set to 10 cm and given a radius of 5 cm. To simulate a tumor, a block of PVC with a higher hardness value and different color is inserted in the phantom. The most common size for a liver tumor is in the range 1-3 cm range according to the research of [38]. Multiple tumors are placed in the phantom. This gives options to create test scenarios with different tumor sized. The phantom can be seen in Figure 3.5. Small PVC spheres were molded to represent tumors. For the main body of the phantom, a beaker was used as mold. The PVC was heated and mixed with a 20% softener to create a softer base material for the phantom. Once the mixture cooled, the tumors were placed inside the still liquid PVC mixture. The phantom solidified over time.

Table 3.1: Material properties comparison [36]

	Attenuation	Young's modulus	Shore hardness	Needle insertion	Durability
Agar	+++	+	?	+	+
Gelatin	+++	+++	?	+	+
Polyvinyl chloride	++	+++	+++	++	+++
Silicone	+	++	++	++	+++
Polyvinyl alcohol	?	++	+++	+++	++
SEBS	+	+	+	+	+++

SEBS = styrene-ethylene-butylene-styrene co-polymer; +++ = best; ++ = suitable; + = worst; ? = unknown.
Each material property was compared with the values for biological tissue and scored on its closeness to this value.
Durability includes storage requirements, resistance to cracking/deformation and shelf life.

Figure 3.5: The made phantom from PVC. The blue parts are the tumors.

3.3 System Description

3.3.1 Interfaces

The desired system has a lot of different parts which run on a lot of different types of systems. All systems have to communicate in a certain way. The interface diagram can be seen in figure 3.6. Magic Leap 2 has its own integrated computer on which the Unity AR application runs. Using the ROS TCP connection library, a connection between Unity and the ROS environment is made. By running the server endpoint in the Ubuntu environment, a connection is made utilizing a TCP connection. The Magic Leap becomes a client to this server. The Ethernet connection is achieved by using the USB-c port on the Magic Leap. Using this in combination with a USB-C to Ethernet adapter, a ROS connection between the two systems is made. For the 2D- and 3D screen setup, a Windows computer running the unity applications can communicate in the exact same way. Connecting the Omega 6 to the Ubuntu environment is done using a USB connection. And finally, communication with the Franka is done using ROS. All connection are real time capable and enable the system to function with low delays, satisfying that requirement.

3.3.2 Virtual Environment

The virtual environment provides all the visual feedback for the surgeon. The intention for this environment is to provide this information in the clearest way possible. The implementation of this environment is different for the different modalities.

AR

In this setup, the user performs the remote surgery using an AR environment. An AR environment is characterized by having digital information displayed in the physical world. For remote surgery, the patient is not near the surgeon. Displaying information overlaid on the patient is not an option. Still, there are benefits to creating an AR environment. A fully digital representation of the patient can be made as if they were in the room. Any additional information such as the status of the operation can be rendered in the same environment. An advantage This allows them to maintain a connection to the real world and interact with other devices or people in the room. In contrast, VR can diminish spatial awareness and increase the risk of motion

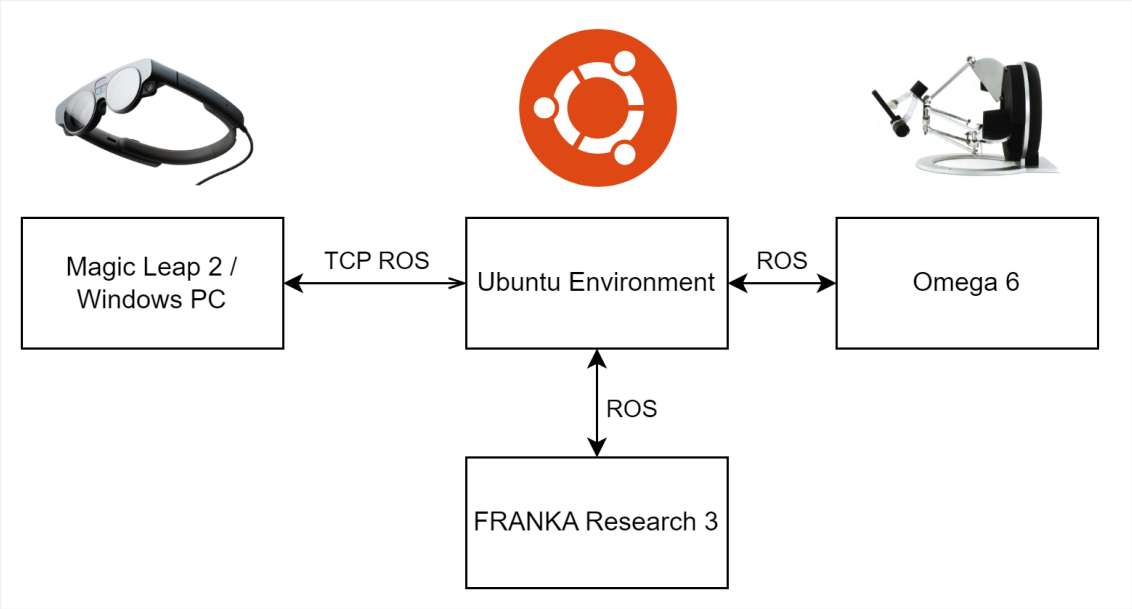

Figure 3.6: The interface model between the different systems. Differences between AR and non-AR setup are minimal. Can be interchanged between the Windows PC and the Magic Leap 2

sickness due to its immersive nature [39]. Benefits over a simple screen is that it can display objects and information in the world, which can give benefits with depth perception, and a better general feeling of where things are compared to each other. More interactive controls can be implemented using specific AR controllers or alternatively hand controls.

2D Display

The 2D implementation is made using a standard Unity project. This consist out of scene with a standard 2D rendering camera. In the AR environment the digital patient can be placed anywhere in the world, in this modality the digital patient is rendered to the screen. The same model and visual indicators that are used in the AR environment can be reused here. But instead of a 3D representation, they are viewed through one perspective, without additional 3D information. Utilizing different viewpoint through camera translation and rotation can still give us different angles. The intention is to make the AR and non-AR environment similar visually.

3D Display

This application is rendered on the Barco 3D display. Compared to the 2D implementation, the main difference is the addition of a 3D camera in the scene. With a regular rendering camera, only the nearest object rendered matters, at least for opaque objects. With a 3D camera, the distance to the camera matters for the 3D rendering. In Figure 3.7 the 3D camera in Unity can be seen. The area between the purple lines shows the 3D rendering space. The closer an object is to the 3D camera edges, the higher the disparity of the interlaced images, resulting in a greater 3D effect. Because a depth camera is integrated into the display, motion parallax is implemented as well. Users can move their head and the object will move as seen from that viewing angle.

3.3.3 Visual Indicators

Before implementing the different modalities, let's address a common element for all of them: visual indicators that assist users in aligning the needle. Effective visual indicators depend

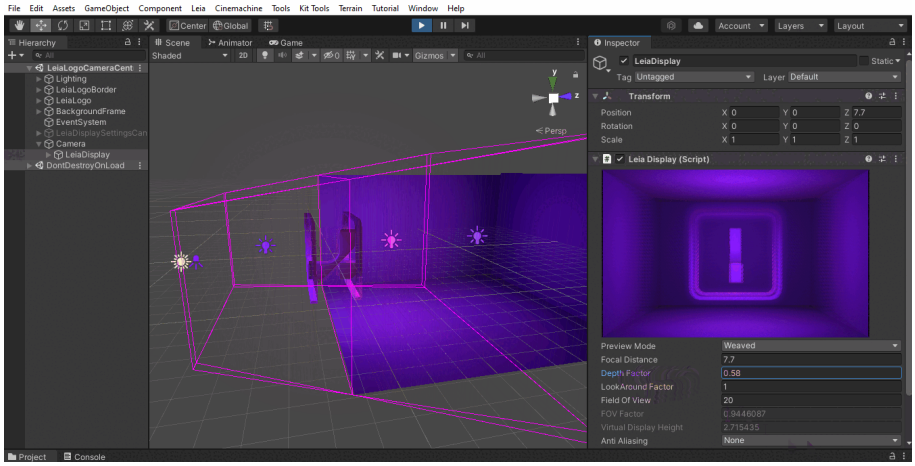

Figure 3.7: 3D camera in Unity using the Leia SDK for Unity. The rendering space is represented by the purple outlines. Objects that are closer to the near edge will appear to pop out of the screen. Object that are closer to the far edge will appear to be inside the screen. [40]

on understanding what information is important, when it is important, and how it should be displayed. In Table 3.2 a list is made of possible useful visual information.

Through iterative development, different methods for displaying visual indicators were tested, revealing the significance of where information is presented. For instance, in an earlier version of the AR environment, important positional data was shown on floating screens. But since it was floating in space, or in a corner of the screen, the user's gaze was divided between two important pieces of information. Ideally, users need to see needle movement directly in the needle model, along with an indicator for guidance. A solution in this case is to show information in the place where it is used. In the second iteration, which can be seen in figure 3.8 the crosshair is placed directly on the incision point. This crosshair provides critical information about the needle tip position. The red and cyan line show the alignment in the x and y directions, respectively. By perfectly aligning them with the crosshair, proper alignment is reached. This system is also reused for accurately inserting onto the tumor. This has multiple benefits, the user can naturally see the interaction between the indicator and the needle. The user does not have to split his/her gaze between the visuals. However, a potential drawback is information overload if not implemented carefully, and the risk of blocking other important information, such as the liver model and veins. To mitigate some of these effects, unnecessary indicators are removed once they are no longer needed. The crosshair for the incision is no longer necessary once the needle is inserted, therefore it is removed at that point. Depth is shown with the same indicator by having a blue circle increase in size depending on the distance. An empty indicator means the needle is far away, and a full circle indicates that the tip is right on top of the target. This idea was inspired by Heinrich et al. [12].

Additionally, a line from the tip of the needle to the target point is shown, this clarifies both the position of the needle tip and the target point, while indicating the desired path of the needle. This line helps users determine if the needle is properly aligned with the path vector. Outlines of relevant organs are shown. Giving users a better feel for their position. Due to the novel nature of the haptic feedback, an indication was given of what control mode the user is in. Patient information, robotic arm status, and remote side footage were excluded from this implementation. The phantom does not accurately represent a patient, making remote footage less useful and costly in terms of bandwidth. While robotic arm status is crucial in real-world applications, it could complicate testing for this group. The same reasoning applies to displaying patient information.

Table 3.2: Description of possible visual info

Visual info	Units	Visual indicators	Importance	Feasibility
Depth	scalar mm	Text Trace pointer Bar Side view	++	+
Needle angle	quaternion or euler angle	Text Trace pointer Side view Relative to trajectory	+	+
Needle tip position	point mm	Text Floating point in space Crosshair indicator Side view Trajectory deviation line	++	+
Patient info	~	Text Images Video Graphs data	-	++
Planned trajectory	vector	Floating Line Side view	+	++
Incision point	point mm	Point Crosshair marker	+	++
End point	point mm	Point Crosshair marker	+	+-
Outlines of Tissues	mesh	Shown outlines Danger zones Transparent model	+-	-
Robotic arm status	flag	Text Model of arm in scenario	–	+
Remote side footage	video	Screen with video	+-	+-

3.3.4 Unity implementation

As previously mentioned, the ROS communication is implemented by using the ROS TCP Connector library. By utilizing this library, a ROS connection can be made using TCP. To achieve this TCP connection with the Magic Leap, it needs a network connection to the Ubuntu environment. By utilizing its USB-C port and a USB-C to Ethernet adapter, a wired network connection is achieved. In this connection, the Ubuntu serves as server, and the unity application as client.

The Unity application serves mostly visual information to the user. In ROS all the relevant transforms are kept track of in the "/tf" topic. Using this topic, all relevant transforms can be kept track of in unity. Based on the transform, the models can be placed at the appropriate places at the appropriate time. A model can subscribe to a transform and follow its direct pose in real time.

Furthermore, our AR environment has real life coordinates in which the models are placed. These models include the phantom, which can be seen in Figure 3.9. By defining an origin frame, the transform tree can be placed relative to this origin frame. The models can be moved to the desired pose by translating and rotating the base of the transform tree. Furthermore, scaling options are implemented. These are implemented using Unity's transform system, in which the scaling of a parent Game Object causes all "Children" to scale with it. When this is done for the base of the transform tree, the distances between them increase linearly with the scaling factor. Scaling and rotating require a pivoting point, by default this is the origin position. This is not ideal for us, since the base of the robotic arm is on the origin. Therefore,

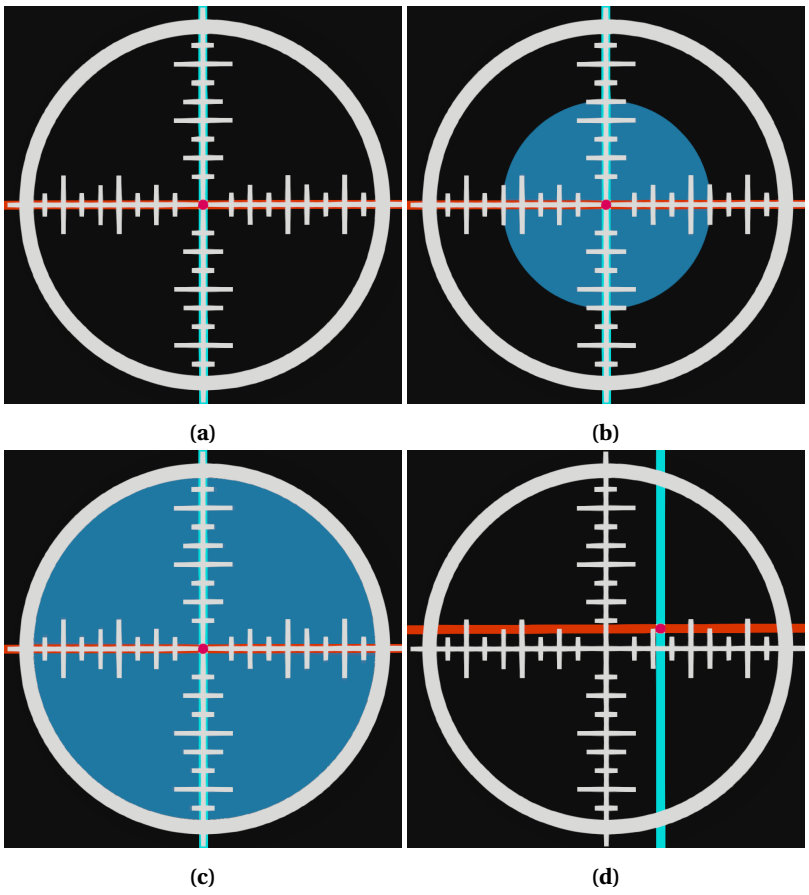

Figure 3.8: Showing the crosshair for different needle positions. In (a), the needle is perfectly aligned but far away. For plot (b) the tip is close to the incision. In (c) the needle is right on top point. In (d) a misalignment can be seen.

the rotating and scaling point is set to be the incision point. This implemented by calculating the movement of the incision point after rotating/scaling, and then offsetting the base of the transform tree by this amount. Ensuring that the incision point stays in the same position in the "real" AR environment. After testing the system, it was found that better viewing options could be achieved by setting the rotation point to the needle tip once inserted. Options for the user to rotate, translate and scale the scene as desired are provided with the use of a keyboard for the 2D and 3D application. In the augmented reality environment, these are controlled using the magic leap controller. The control scheme can be found in Figure 3.10. User move the model by holding the bumper. When the bumper is held, the movement of the controller is mimicked by the model, e.g. a move to the left coincides with the model moving to the left. Users can scale by holding the trigger. While holding the trigger, moving the controller up increases the size of model and vice versa. Finally, the trackpad is used to rotate the model. Moving along the trackpad rotates the model around that axis (from a world perspective). In an earlier version, rotation was mapped to the rotation of the controller, but this was found to be too hard to control. Some physical rotations with the controller are tough on the wrist. Finally, the menu button opens the menu. In this menu, the scenario can be ended.

For visual guidance, the aforementioned crosshair is rendered on top of the model, right on the incision point. This is achieved through shaders, which are GPU-based programs that manage the rendering of graphics, including handling light, color, and textures. Shaders are highly efficient but difficult to write. Therefore, shaders were implemented using Shader Graph [41], a visual shader creator tool. A custom crosshair shader is used to wrap the crosshair texture

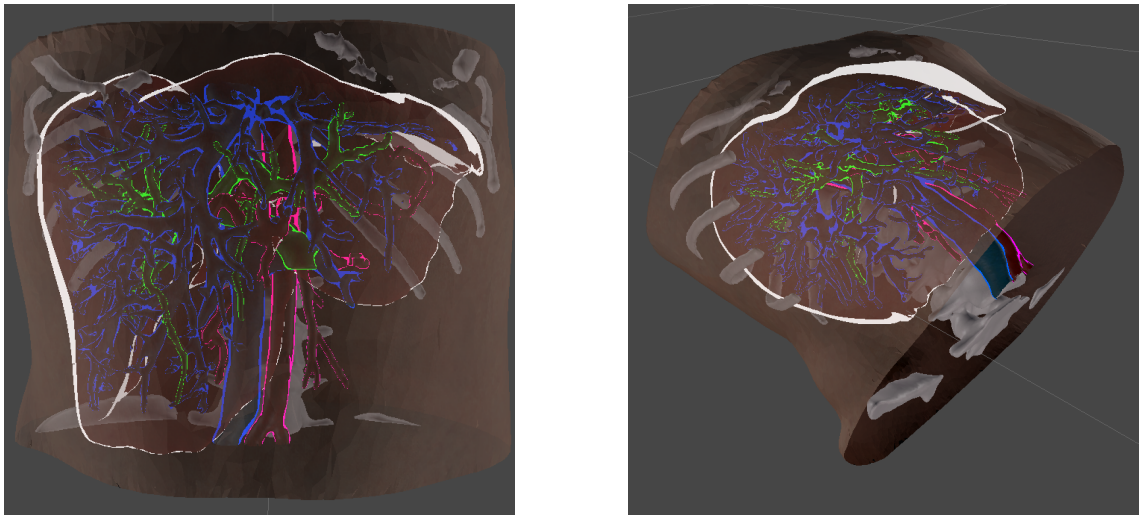

Figure 3.9: The used model representing the patient. An outline shader is applied to the models to give users an indication of the outlines.

Figure 3.10: The magic leap controller with controls for the AR environment.

around the model, matching its deformation. In addition to the crosshair, two navigational lines and a dot are rendered. These elements provide guidance on how the needle aligns with the crosshair, clearly indicating the needle's position relative to the incision point. For measuring the distance to the incision, a circle expands in size based on the distance between the needle tip and the incision point.

To clearly indicate of when the incision is made, these markers are removed when the needle is inserted into the skin. This is defined as when the needle tip reaches the threshold beyond the incision point. Internally, the system checks a very wide cone behind the incision point to measure if the tip is located there. Furthermore, an expanding hole is made in the model of the skin to get a clearer view of the needle and underlying tissue. around the insertion point, a small circle of the skin is still rendered to give an indication of the height at which the needle inserted. Images of the 2D application can be seen in Figure 3.11.

3.3.5 Haptic Feedback

The main goal for haptic feedback in this project is to support accurate needle control. There is no focus on trying to make the force feedback feel like moving an actual needle. Realistic simulating of needle insertion dynamics can be useful for training of novice surgeons, and helping experienced surgeons use their learned expertise. But the ideal outcome of a needle insertion is to insert the needle as precise as possible. The dynamics of needle insertion in an operation are based on physics. The tissue of a human being exhibits specific characteristics that naturally generate particular force feedback during an insertion. Surgeons can learn the re-

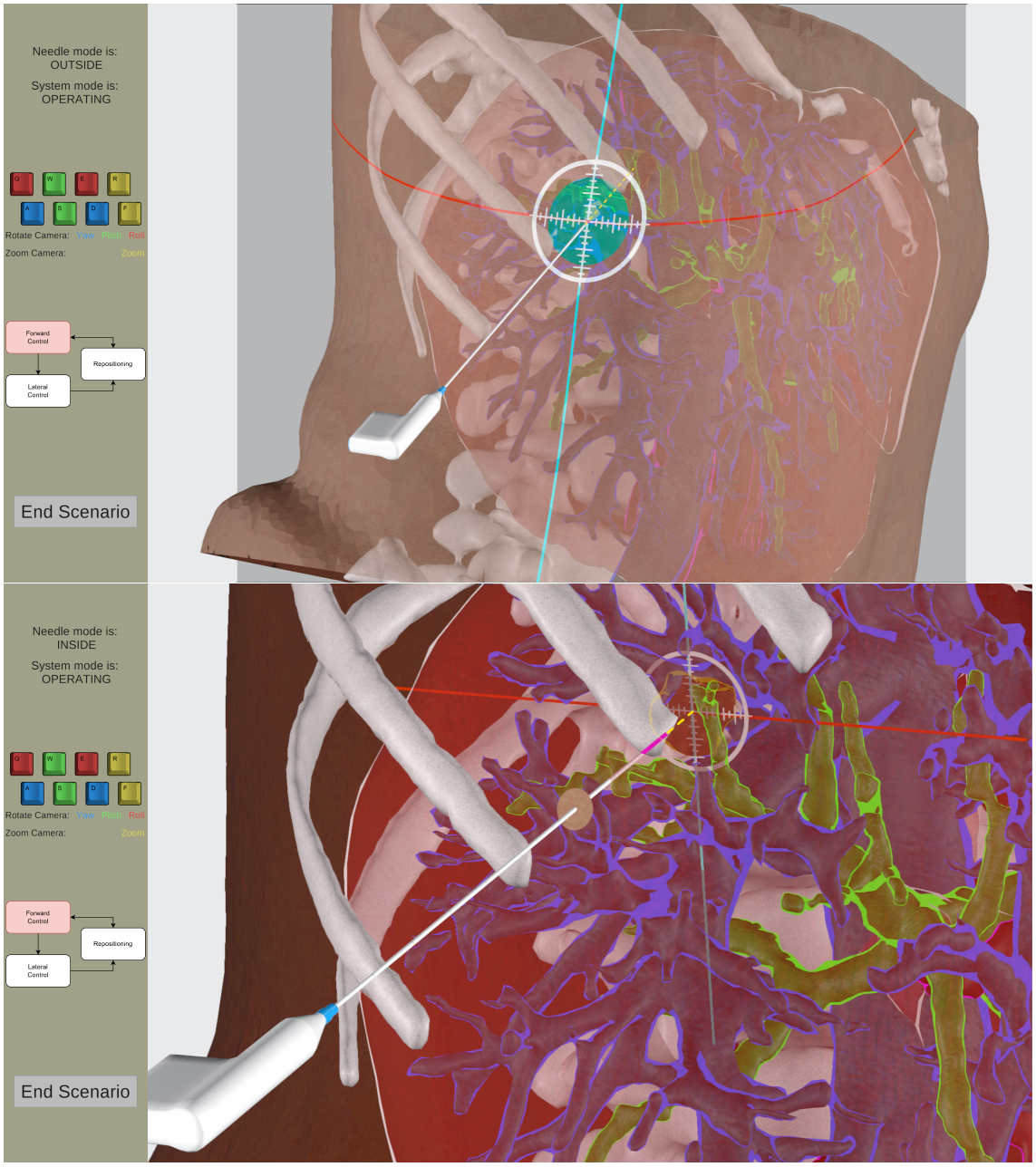

Figure 3.11: The images depict the 2D application in action. In the first picture, the needle is outside, with the crosshair providing information about the alignment and distance of the needle. In the second picture, the needle is inside the tissue. Here the skin is not rendered to give a clearer view, besides a slight area around the needle. This gives information about the rotation point of the needle. The crosshair is reused for aligning with the tumor. The needle can be seen as purple when occluded, a yellow jagged line shows the path from the tip of the needle to the target point and general information can be seen on the left UI.

sponses a needle will have when inserting and understand the meaning behind it. But since it is all physics based, the dynamics of such a surgery are not designed to provide optimal haptic feedback. By utilizing custom force feedback, beneficial dynamics can be designed. Dynamics that provide stability, accuracy, precision and satisfaction. Another issue with realistic haptic feedback is difficulty combining it with sensitivity options. The mapping of the controller to the robot effector is no longer one-to-one, realistic force models can no longer be used, since different distance scaling values are used. Therefore, a non-realistic approach is taken, focused on providing user-friendly precise controls.

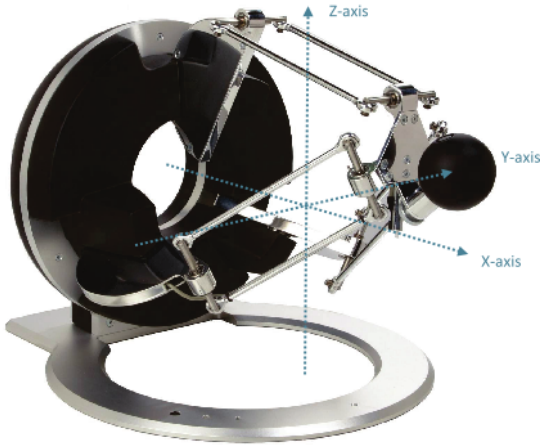

Figure 3.12: The Cartesian coordinate system of the Omega x [42]

.

The haptic feedback is provided by the Omega 6 device. In Figure 3.12 the coordinate system of the device is depicted. Force feedback can be provided in these directions. Additionally, the system can track the rotation of the effector. The system lacks torque feedback. This makes controlling the rotation of the effector hard. It is very easy to accidentally make large rotations without intention, since there is no force stopping the rotation. Therefore, it is opted to not use the rotation measurements for the needle control. Yet, it is still necessary for the user to be able to rotate the needle in certain situations. This leads us to the question: How should the needle move during the procedure?
Key considerations are:

- **Forward Movement**: The ideal needle movement is a smooth forward motion. If the starting position is good, only small adjustments are necessary for precise needle alignment.
- **Lateral Movement**: When outside the tissue, the needle can move laterally without constraint (within reason). Inside the tissue, lateral movement is very constrained, lateral movement to stretch or even damage the skin.
- **Rotational movement**: Inside the tissue, limited rotational movement around the incision point is still possible to fine-tune the needle's position.

These considerations leave us with a good option for pure Cartesian control: When the needle is outside the tissue lateral movement result in lateral movement, when inside the tissue lateral movement results in a rotation around the incision point. In Figure 3.13 this needle control method is shown in 2D. The forward direction of the haptic feedback device can be in the forward direction of the needle. To accompany this needle movement system, a novel haptic feedback control scheme is implemented. The x coordinate is treated as the forward direction and the yz coordinates are considered the lateral direction. Moving in both of these directions at the same time is confusing when rotation is involved, therefore it is chosen to separate the forward and lateral movement. Meaning, a user can only move in one direction at a time.

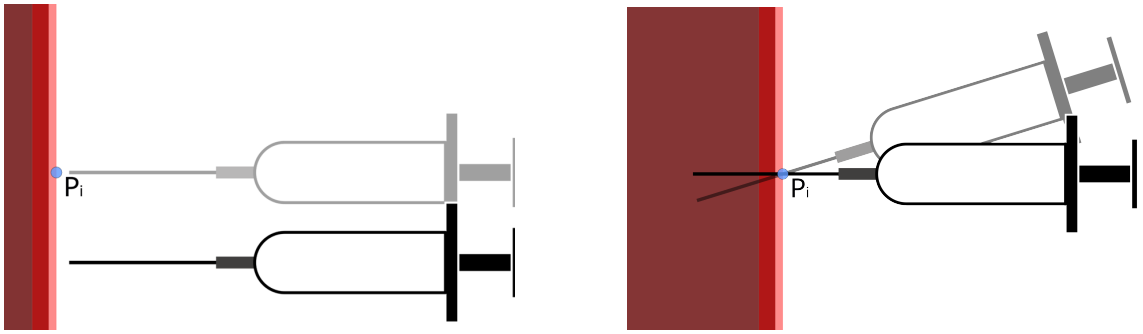

(a) Lateral Needle Movement

(b) Rotational Needle Movement.

Figure 3.13: (a) Lateral needle movement outside the tissue. (b) Showcase of the needle rotating around P_i. The amount of rotation has been exaggerated for this image

Control Scheme

Figure 3.14 shows the control flow diagram of the haptic feedback controller, with state descriptions in Table 3.3. Control of the needle is divided into moving forward along the trajectory and moving lateral. This separation allows for precise control of the needle's movement, while together still providing the full range of motion. Forward control works as follows: The effector tries only allow forward movement. It tries to keep its lateral coordinates zero. This is implemented with the use of a PD controller. This PD controller corrects position errors by pushing the controller back to the center. In the forward direction, a velocity controller is implemented to limit the speed at which a user moves. The velocity controller has a set point of 0, meaning it tries to stop movement. This makes it difficult to make fast movements and prevents accidental slips. It will influence the user to make smoother movements. Internally, the force vectors calculated by these two controllers are added up and become the effective force feedback to the user. If the user wants to move laterally, they have to move the needle beyond a certain lateral distance. The aforementioned PD controller will give a force against this movement, users will only enter lateral control when they apply conscious force in the lateral direction. The lateral controller works the same way as the forward controller, only the PD and velocity controller are switched. The PD controller works in the forward x direction, and the velocity controller along the lateral plane. The PD controller's set point is the x value when lateral control is initiated. The velocity controller works in the plane and applies a force in the opposite direction of the last measured lateral speed vector. Lateral control functions differently inside and outside the tissue. Outside the tissue, rotation of the needle is unimportant. The main focus is getting an accurate insertion. Once inside the tissue, the lateral movement is a rotation around the incision point.

Lateral control is exited by using the button on the effector, entering the ALIGNING state. A PD controller is activated to move the Omega effector back to the center. Once the effector is back in the center, the user can move forward again. During this ALIGNING state, the Omega and robot arm are decoupled, meaning the robot remains stationary while the Omega effector moves.

Due to the Omega's limited workspace, clutching is implemented. When the workspace in the x direction ends, the Omega applies force towards the starting point until it is reached. Once this point is reached, the system enters forward control. The user can move forward once again.

One major benefit of robotic surgery is motion scaling, where small precise robotic arm movements correspond to larger user-side movements [43]. Sensitivity options for forward and lateral control allow precise control as needed.Sensitivity is managed by scaling the local frame measurement with a sensitivity factor. Separate sensitivity factors are used for forward and lateral controls. Low sensitivity is particularly important for lateral control, as the user is fine-

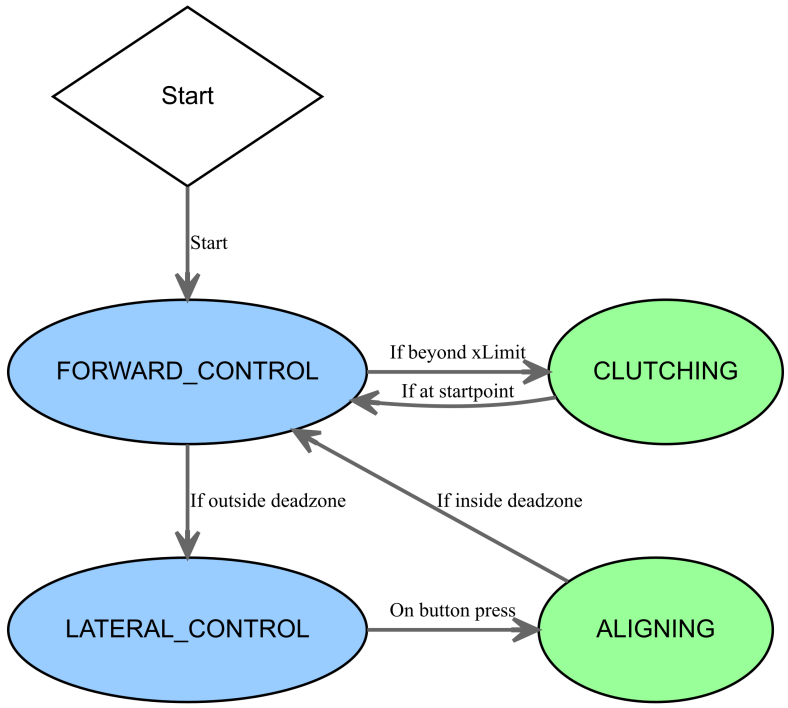

Figure 3.14: The control flow diagram of the haptic feedback controller. In green nodes, the robotic arm and Omega are decoupled.

tuning the needle's alignment. Although these sensitivity options could theoretically be adjustable by the user during the procedure, this feature has not been implemented to not increase the complexity of the system.

Table 3.3: Description of the separate states of the controller.

State	Goal	Leave state conditions	Updates	Coupled
FORWARD_CONTROL	The purpose of the forward controller is to keep the effector on a straight trajectory, it 'locks' the effector in the lateral direction and frees the user in the forward direction	If yz length is outside of set limit ->LATERAL_CONTROL If x position is beyond set boundary ->CLUTCHING	x position	**Yes**
LATERAL_CONTROL	The plane controller allows the user to adjust the trajectory of the needle, by being able to move in the yz directions the x direction is locked	If button on the effector is pressed ->ALIGNING	yz Position Rotation if Inserted	**Yes**
ALIGNING	After the user has made his adjustments he controller needs to move back to the position it entered LATERAL_CONTROL	Effector back in position before entering LATERAL_CONTROL ->FORWARD_CONTROL	-	**No**
CLUTCHING	Due to the limited workspace of the Omega, it is necessary to clutch. This means when the end of the work space is reached control is taken away and the effector is moved back to the start.	Effector back in start position ->FORWARD_CONTROL	-	**No**

Frame Assignment in the Real-world Environment

Some variables and terminology

- $\mathbf{v}_t$: Needle trajectory vector, running from the needle handle to the needle tip.
- $\mathbf{v}_p$: Planned trajectory vector, start point to target point.
- P_c: Needle control point, the pivot point of the needle
- P_{tip}: Needle tip point
- P_t: Target point, the final point of the planned trajectory.

- P_s: Start point, intended starting point of the needle origin.
- P_i: Incision point, the point on the planned trajectory that intersect with the skin.
- R_n: Rotation matrix, defining the orientation of the needle.
- L_{needle}: Length of the needle
- L_{offset}: Set starting offset from the incision point, the distance the needle has to travel before inserting.

The needle trajectory $\mathbf{v}_t$ is defined as the vector from P_c to P_{tip}. It runs perfectly along the shaft of the needle. Control is exerted from the needle origin, which serves as the pivot point for the needle's rotation.

the planned trajectory is defined as the vector from the incision point P_i and the end point P_e, both set before the procedure. The start point P_s is set by going backwards on $\mathbf{v}_p$ from the incision point. One needle length plus a little extra along that result in the values for P_s. At the initiation of the procedure, the needle handle is positioned at P_s, aligned with the planned trajectory. The robotic arm position starts at P_s.

This starting rotation matrix is calculated using the Gram-Schmidt process[44]:

1. **Initialization**: Normalize the known basis vector $\mathbf{v}_1$ to obtain $\mathbf{u}_1 = \frac{\mathbf{v}_1}{\|\mathbf{v}_1\|}$.
2. **Construction of Second Vector**: Choose an arbitrary vector $\mathbf{v}_2$ that is not parallel to $\mathbf{u}_1$. Subtract the projection of $\mathbf{v}_2$ onto $\mathbf{u}_1$ from $\mathbf{v}_2$ to obtain an orthogonal vector $\mathbf{u}_2$.
3. **Normalization**: Normalize $\mathbf{u}_2$ to obtain an orthonormal vector.
4. **Calculation of Third Vector**: Take the cross product of $\mathbf{u}_1$ and $\mathbf{u}_2$ to obtain $\mathbf{u}_3$, which is orthogonal to both $\mathbf{u}_1$ and $\mathbf{u}_2$.
5. **Construction of Rotation Matrix**: Arrange the orthonormal vectors $\mathbf{u}_1$, $\mathbf{u}_2$, and $\mathbf{u}_3$ as columns of the rotation matrix and normalize them.

The known basis vector is the planned trajectory vector, which normalizes to get $\mathbf{u}_1$. Choose $\mathbf{v}_2 = (0,0,\alpha)$, for $\alpha > 0$ ensures that $\mathbf{u}_3$ lies in the plane defined by $\mathbf{v}_1$ and $\mathbf{v}_2$.

$$\mathbf{u}_2 = \mathbf{v}_t \times \mathbf{v}_{P_s \to P_i} \tag{3.1}$$

Note that when the trajectory and our defined vector have the same alignment, this process will fail, since the cross product of 2 vectors in the same direction is zero.

In the needle coordinate frame, $\mathbf{v}_t$ aligns with the x-axis. The y and z components are defined to point up for a comfortable robotic arm position.

$$(P_1 = P_e + (0,0,\alpha) \tag{3.2}$$

$$\mathbf{v}_y = \mathbf{v}_t \times \mathbf{v}_{P_s \to P_1} \tag{3.3}$$

$$\mathbf{v}_z = \mathbf{v}_t \times \mathbf{v}_y \tag{3.4}$$

With arbitrary $\alpha > 0$. These vectors, when normalized, form the basis vectors of our start rotation matrix:

$$R_n = [\hat{\mathbf{v}}_x, \hat{\mathbf{v}}_y, \hat{\mathbf{v}}_z] \tag{3.5}$$

Now all the relevant coordinate frames and points have to be placed. Starting with the robotic arm, which in this case has two relevant frames. The base link frame, positioned at the robot origin, and the robot end effector frame T_{RE}. All links in between are only relevant for controlling the robotic arm, which the robotic arm controller will manage. The choice is made that the base link frame is equal to the world frame, meaning it is at the origin of the robot scene. Next, the phantom is placed in the scene. The phantom is given its own coordinate frame, since it has its own pose compared to the base link. In this frame, two points of interest are placed. The predefined target point P_t and the incision point P_i. In surgery, these would be planned

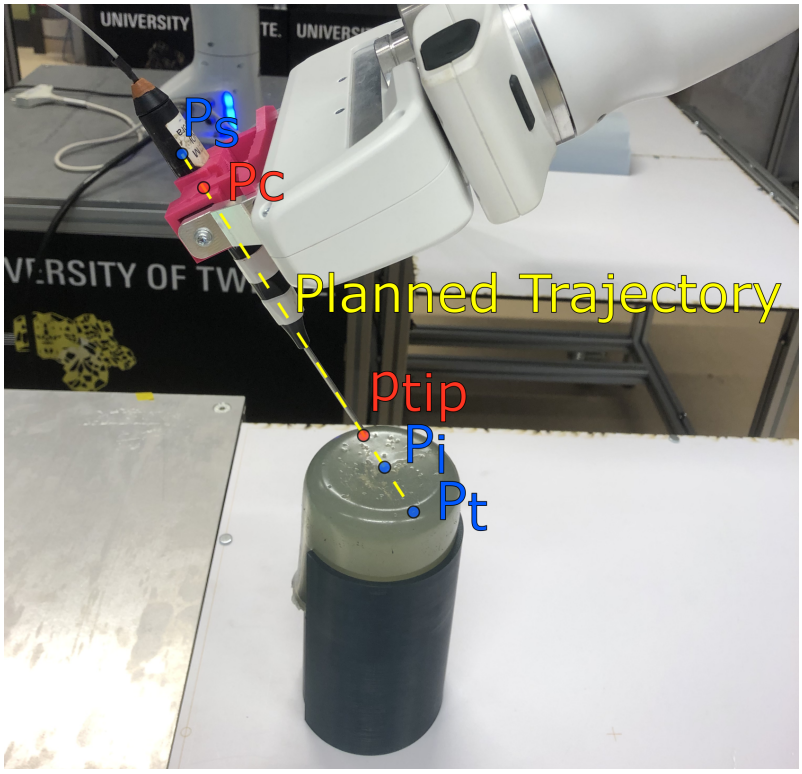

Figure 3.15: Highlighting points in the robot scene. Blue points are in the phantom frame, red points are in the world frame

before the operation takes place. P_t represents the targeted point in the tumor, usually the center. The P_i describes the intended point of penetration on the skin. Since the phantom is a constant, these can be defined as static points in the phantom frame. Using these two points, the desired starting point P_s of the needle can be calculated. It can be calculated with simple vector math:

$$\mathbf{v}_p = P_i - P_t \tag{3.6}$$

$$P_s = P_i + \hat{\mathbf{v}}_p * (L_{needle} + L_{offset}) \tag{3.7}$$

The direction vector from P_t to P_i is calculated, and used to set the starting point in the same line at the distance $(L_{needle} + L_{offset})$ from P_i.

The needle is controlled by the measurement of the Omega 6. The movements of the Omega effector are measured in its own frame T_{omega}, recall Figure 3.12. The position of the Omega effector is called P_{input}. To actually control the end effector in the remote scene, there has to be some conversion between the Omega measurement and the robot effector position. This is achieved by placing T_{omega} in the robot scene. This is written down as ${}^0T_{omega}$ with zero, indicating it is in the world frame. At initialization, the translation of ${}^0T_{omega}$ can be set to be equal to ${}^0P_s$, the world position of the previously defined P_s. The rotation of ${}^0T_{omega}$ is set to the previously calculated rotation matrix R_n

Using T_{omega} the desired robot effector frame is set by calculating the input:

$${}^0T_{RE} = {}^0T_{omega} * P_{Input} \tag{3.8}$$

There are two additional steps in the process, that occasionally have to be taken. As discussed in the previous chapter, to go beyond the workspace of the Omega, clutching has to be implemented. In the clutching operation, the Omega effector returns to the origin while decoupled.

${}^0T_{RE}$ should stay the same before and after clutching, otherwise the robot effector would make an unintended movement. Therefore, ${}^0T_{omega}$ is updated after coupling to ensure this. It is updated in such a way that equation 3.8 has the same result for the new P_{Input} value.

There are 3 types of implemented coupling and decoupling: Clutching, Aligning outside tissue, Aligning inside tissue.

Clutching is the simplest, when decoupling the frame ${}^0T_{omega}$ is set equal to ${}^0T_{RE}$. Now since the Omega effector is back at the origin P_{Input} is zero.

For aligning outside tissue, the Omega effector offset in the lateral direction is taken and T_{omega} is translated in that local direction. The Omega effector is pushed back to trajectory control such that the values for y and z are set to zero.

For aligning inside tissue, the needle rotates around P_i. Making the procedure a bit more complex First, the rotational movement of the needle has to be described. The desired pose can be calculated using the following steps:

$$\mathbf{v}_1 = {}^{omega}P_{input} - {}^{omega}P_{inc} \tag{3.9}$$

$$\mathbf{v}_2 = [x_{input}, 0, 0] - {}^{omega}P_{inc} \tag{3.10}$$

^{omega} represents that it is expressed in the local frame of ${}^0T_{omega}$.

$\mathbf{v}_1$ represents the vector from ${}^{omega}P_{inc}$ to ${}^{omega}P_{input}$. $\mathbf{v}_2$ is the vector between the point from which plane control was entered to ${}^{omega}P_{inc}$. These two vectors have an angle between them, which can be calculated using the dot product:

$$\mathbf{v}_1 \cdot \mathbf{v}_2 = |\mathbf{v}_1||\mathbf{v}_2| cos(\theta) \tag{3.11}$$

$$\theta = cos^{-1}\frac{\mathbf{v}_1 \cdot \mathbf{v}_2}{|\mathbf{v}_1||\mathbf{v}_2|} \tag{3.12}$$

The axis of rotation is equal to the cross product:

$$u = \mathbf{v}_1 \times \mathbf{v}_2 \tag{3.13}$$

With the rotation axis and the angle, the new rotation of the needle can be calculated using the Rodriquez formula [45]:

$$\mathbf{R} = \cos(\theta)\mathbf{I} + (1 - \cos(\theta))\mathbf{u}\mathbf{u}^T + \sin(\theta)[\mathbf{u}]_\times \tag{3.14}$$

with skew matrix $[\mathbf{u}]_\times$

$$[\mathbf{u}]_\times = \begin{bmatrix} 0 & -u_z & u_y \\ u_z & 0 & -u_x \\ -u_y & u_x & 0 \end{bmatrix} \tag{3.15}$$

Using R to rotate $\mathbf{v}_1$ gives:

$$\mathbf{v}_3 = R * \mathbf{v}_1 \tag{3.16}$$

Using $\mathbf{v}_3$ our desired needle position P_{needle} is found with:

$$P_{needle} = P_i + \mathbf{v}_3 \tag{3.17}$$

The needle rotation is found by rotating ${}^0R_{omega}$ by R. The variables are shown visually in Figure 3.16.

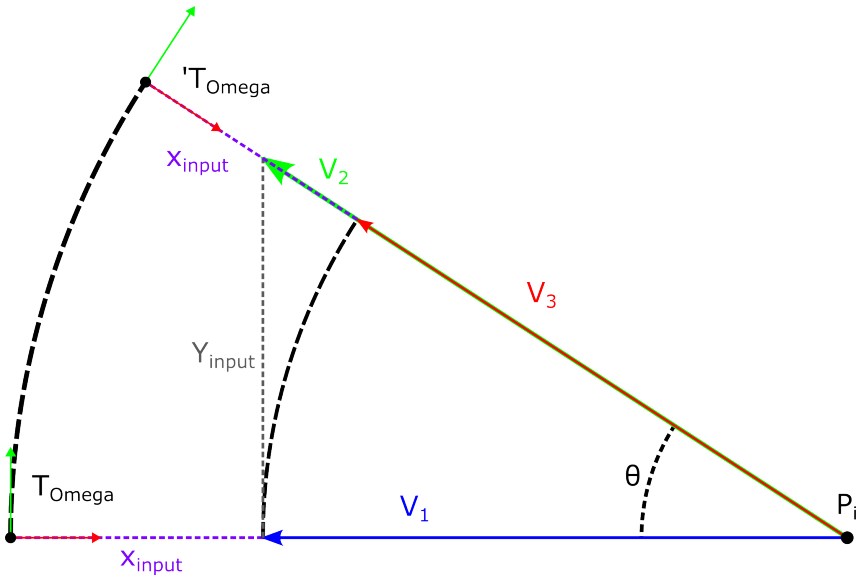

Figure 3.16: 2D representation of rotating the needle. In this case, the lateral input only has a y value, resulting in a 2D rotation. ${}'T_{omega}$ represents the new frame after decoupling.

Decoupling for this is similar to the previous methods. The new ${}^0T_{omega}$ is equal to the needle pose ${}^0T_{needle}$ shifted backward along its own x-axis. This can be accomplished by multiplying it with a translation matrix:

$$T_x(x_{input}) = \begin{bmatrix} 1 & 0 & 0 & -x_{input} \\ 0 & 1 & 0 & 0 \\ 0 & 0 & 1 & 0 \\ 0 & 0 & 0 & 1 \end{bmatrix} \tag{3.18}$$

$${}^0F_{omega} = T_x(x_{input}) * {}^0F_{needle} \tag{3.19}$$

3.3.6 Robot Control

Control of the Franka arm was initially implemented using the provided impedance controller of the Franka library. After testing, it was observed that the steady state position errors were too large(±1cm), therefore it was decided to use a different library. The MoveIt library is a widely used software for motion planning[46]. Operating a robot arm is done in two steps, first the path from the current pose to the set pose is planned. According to this plan, the robotic arm is moved according to the calculated plan. The planning problem is solved by a sampling based motion planner. A sampling based motion planner solves the high complexity problem of the movement of the robotic arm, which consists out of 7 links. One issue with such planners is that calculating the optimal path can take a relatively long time. Another disadvantage, the robotic arm has no motion at the start and end of each plan. This creates a jittery motion instead of a steady motion. The major upside is that the accuracy is very good, being able to reach poses with sub mm errors. Therefore, it is opted to use the MoveIt implementation over the impedance controller. Future projects should consider finding a different library or building their own controller.

The needle is held in the gripper of the Franka, which can be seen in Figure 3.17. The handle of the needle, which is the intended control point, is slightly below the gripper. This offset has to be compensated. There are two solutions to this problem, one is to add a link in the transform tree of the Franka representing the needle and use that as the end effector. Another is to take the needle to gripper transformation into account when setting the robot effector position. The second option is implemented.

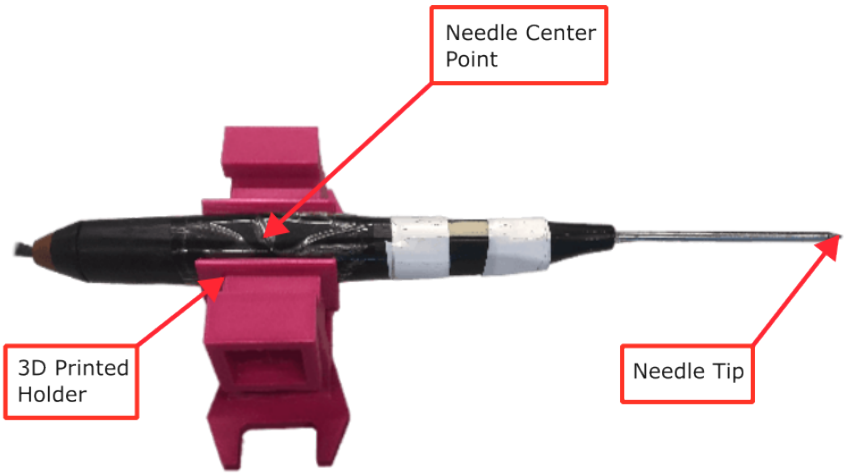

Figure 3.17: The used needle held by a 3D printed part.

The robotic arm is place on the incision point and this information is used to place the phantom in the scene. The phantom is placed in a 3D printed holder that can be placed in a consistent place on the platform. Guaranteeing it is always on the same position compared to the robotic arm. Given the pose of the phantom, the predetermined incision point and target point have world coordinates. Furthermore, as previously discussed, the starting pose of the needle can be determined using those two points and the length of the needle. The complete setup can be seen in Figure 3.18.

3.4 Setup

3.4.1 Test Setup

Participants will perform a simulated needle insertion procedure using an Omega 6 controller to manipulate a Franka robot. The goal is to accurately insert a virtual needle into a phantom using the three visualization methods: Magic Leap, a 3D display, and a 2D screen. The user setup for the non-AR modalities can be found in Figure 3.19. The User setup for the AR modality is found in Figure 3.20

A comparative analysis of the modalities can be found in Table 3.4. For this, a start screen is made so that between tests the user can switch to the right scenario. The start screen can be seen in Figure 3.21. For each modality, 3 different scenarios are performed. In these different scenarios, the orientation and position of the target and incision point are different compared to the model. The scenarios are the same across the modalities. A tutorial is used to introduce users to the system and experiment. In the tutorial, the controls of the Omega are disconnected from the robotic arm, ensuring that users can try the system safely. The phantom is set up at a position in front of the Franka, and is manually registered. The phantom holder is locked on the bottom late, to ensure it doesn't move between experiments. After the phantom pose is determined, all other values are updated automatically. Control is then handed over to the subject. The subject can make modifications to the setup according to his preference, e.g. moving the camera to a comfortable place. After that, the test is performed and the user can perform the surgery by controlling the needle using the Omega. On the start, a little bit of a random

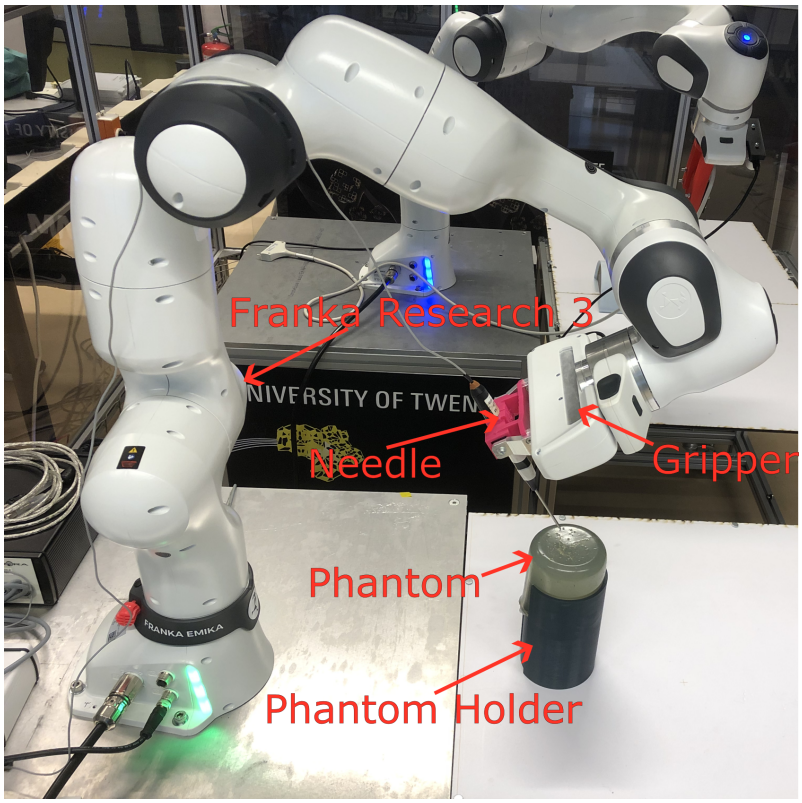

Figure 3.18: Image of the robot setup with the phantom

Table 3.4: Modality comparison.

Modalities	2D display	3D display	AR
Haptic feedback device	Omega 6		
Engine	Unity		
Needle actuator	Franka Research 3		
UI	Screen UI		AR UI
Display device	Barco Display		Magic leap 2
Visualization technique	2D	Autostereoscopic 3D	AR HMD
Environment control	Keyboard Mouse	Keyboard Mouse Head movement	Magic Leap controller
Visual Indicators		Crosshair Surgical path vector Model modifications	

offset is performed on the needle, such that the users are forced to align the needle. Furthermore, there is slight noise on the target point, make it move in determined direction based on insertion depth. The test ends when the user is satisfied with his needle placement. The final position of the needle tip is registered and used as a result. To summarize:

Procedure

1. **Setup:**
   - The relevant modality and scenario are loaded.
   - Participants can adjust the camera position for optimal viewing.
2. **Task Initiation:**
   - The experiment begins with a random offset of the needle, requiring participants to realign it.
   - A slight, controlled movement is introduced to the target point during insertion, effectively causing a slight movement of the tumor.
3. **Task Execution:**
   - Participants control the needle using the Omega 6 to reach the target point.
   - The task ends when the participant is satisfied with the needle placement, and they press a button on the UI.
4. **Data Collection:**
   - Needle tip position is recorded during the procedure, in post-processing the target and incision accuracy is determined.
   - When the user presses the end scenario button, the time is stopped.
   - The system is reset so that the next scenario can start, if it was the last scenario of the modality the users fills in the according survey and the next modality is prepared.

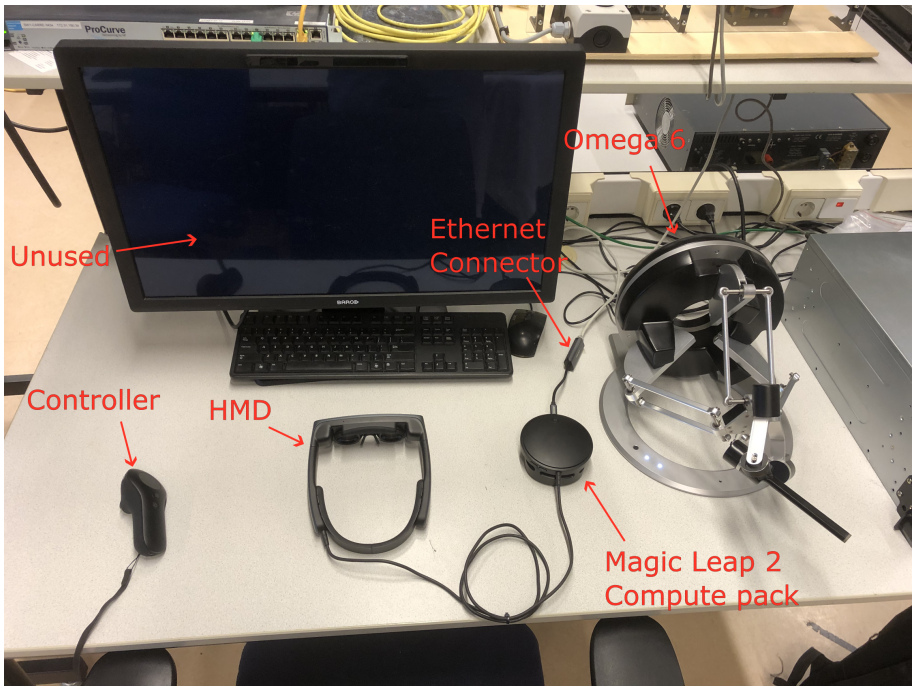

Figure 3.19: Image of the setup where the user will perform the AR modality experiments

3.4.2 Measurements

In Table 3.5 the comparison factors are written down. Consisting of accuracy, time and usability. These same factors are used in other studies [12] [37] to determine system performance. Accuracy is important since it determines if an operation is successful, if the offset is beyond a threshold then the insertion can fail. The time measures if the insertion is performed in a

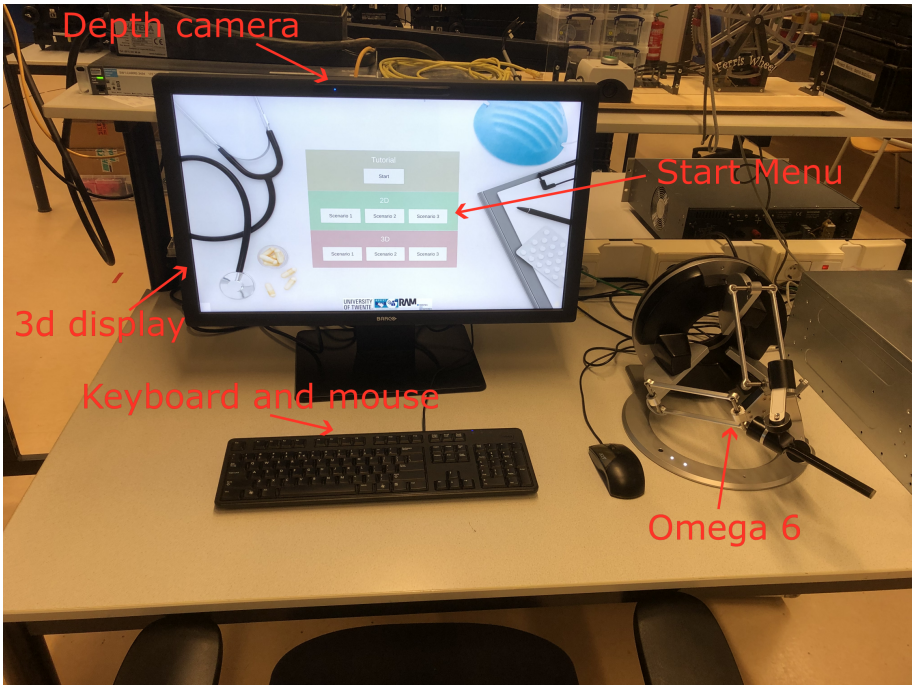

Figure 3.20: Image of the setup where the user will perform the non-AR modality experiments.

Figure 3.21: The start screen of the application. Once users are done with a scenario, they are returned here to select the next scenario (for 3D and 2D).

suitable time frame. Usability measures if the system is liked by the subjects, and that it doesn't cause any discomfort. A system with a low usability is unlikely to be used regardless of performance increase. Comparing the different visual devices in these factors can help to rank them using objective values. This can give evidence towards potential benefits of a device over the others. Accuracy is measured by the measuring the tip position over time during the test. Based on the position of the tip during the test, the total accuracy is determined. The needle tip is measured by two separated entity, one by taking the measurement of the Franka end effector pose. The transform to the needle tip is static to the end effector, assuming the needle doesn't move during the test. A second measurement comes in the form of the EMT tracker system. The total accuracy is determined by going through the measured data and determining the offset to the incision point and the target point. Shifts and deformation of the phantom are not taken into account for the accuracy in this test. Time starts when the user moves the needle and stops when the user ends the scenario. Usability is measured through surveys and is explained in depth in the next chapter.

Validation metrics	**Factors**	**Measuring Method**
Accuracy	Incision Error Targeting Error	Needle tip position measurements
Time	Time to complete insertion	Integrated timer
Usability	Usability of the System	Surveys

Table 3.5: Evaluation Criteria and Methods

Surveys

An element that is hard to measure but very crucial is the usability of a system. Usability is subjective in nature. An attempt to measure it in an objective way is to use surveys. It is opted to use a standardized survey format. This format is the SUS scale[47]. This widely used survey format is composed of 10 questions with a Likert scale. This gives a generalized measurement of usability. The standard questions of the SUS scale can be seen in Table A.1. The questionnaire is taken 4 times. 3 times for each of the modalities and once for the haptic feedback system. The questionnaire is modified to replace system with: "Augmented reality", "3D display", "screen" and "haptic feedback". The surveys are taken right after the testing of that modality. and the haptic feedback after the entire test.

There are other factors that are measured with surveys. Factors such as age and experience. These are measured using a pre-test survey, the questions of which can be found in Table A.2. These factors are captured to discover possible correlations. If, for instance, it is observed that persons with experience in certain elements performs generally better, then this can be an indication of learning curve issues in the test.

After testing, open-ended questions are asked relating to possible remarks and possible improvements. Finally, the respondent is asked to favor an environment. These questions can be found in Table A.3

4 Results

This chapter presents the findings from the user studies, detailing the data and key results.

4.1 Participants

A total of 12 participants aged 24-32 participated in the study. The group consisted of technical students and university researchers with varying levels of eyesight and experience with AR and haptic feedback. One subject was color-blind. Some of the participants had prior experiences with AR and haptic feedback. The full data about the range of subjects can be found within the appendix.

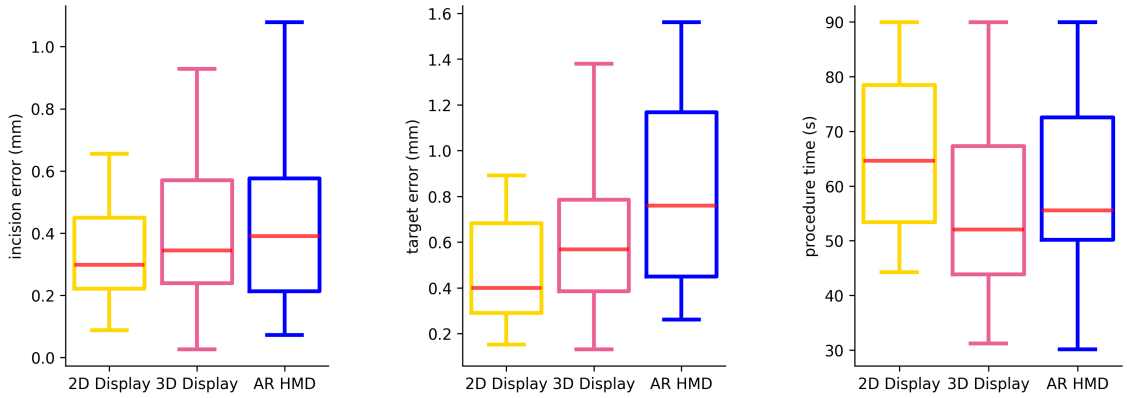

(a) The incision error:
2D: mean of 0.37 mm ± 0.24 mm
3D: mean of 0.40 mm ± 0.25 mm
AR: mean of 0.55 mm ± 0.62 mm

(b) The target error:
2D: mean of 0.81 mm ± 1.12 mm
3D: mean of 0.75 mm ± 0.77 mm
AR: mean of 1.39 mm ± 1.73 mm

(c) The procedure time:
2D: mean of 66.04 s ± 13.39 s
3D: mean of 56.50 s ± 17.19 s
AR: mean of 61.51 s ± 17.95 s

Figure 4.1: Box plot of the measured performance metrics

4.2 Performance Metrics

The results were calculated after completion of the study. The incision and targeting error were computed as discussed previously. One-way within-subjects ANOVA was performed on the collected data. The results are summarized in Table 4.1. Statistical significant result were found for the procedure time with $p < 0.05$ significance. Box plots of the results can be seen in Figure 4.1. Outliers were removed from the box plot to keep the y-axis a small range. These were still taken into account for the ANOVA testing and the calculation of the mean and std.

Table 4.1: Results of ANOVA testing with $p < 0.05$. Collected data from 108 samples per variable, 36 for each modality. 12 subjects had 3 results for each variable

Variable	df	F	p	Figure
Incision error	3	1.97	0.145	4.1a
Target error	3	2.75	0.0685	4.1b
Procedure time	3	3.09	0.0499	4.1c

4.3 User Study Results

The usability test was taken after 3 trials which each modality. The results can be found in Table 4.2. The mean and deviation SUS score of each of the modalities can be seen. The score is calculated for each user with the following progress:

- Convert odd-numbered question responses to a 0-4 scale by subtracting 1 from the original score.
- Convert even-numbered question responses to a 0-4 scale by subtracting the original score from 5.
- Calculate the sum of the converted scores for odd-numbered questions, denoted as X.
- Calculate the sum of the converted scores for even-numbered questions, denoted as Y.
- Compute the SUS score using the formula:

$$\text{SUS score} = ((X - 5) + (25 - Y)) \times 2.5$$

Generally, scores of minimally 60 are considered to be acceptable and scores in the 80s are considered to have excellent usability[48]. How participants answered the survey questions is visualized in Figure 4.3 in combination with the questionnaire in Table 4.3. In the radar chart, responses to the negative even-numbered questions were inverted from a 1-5 scale to a 5-1 scale. This adjustment ensures that higher numbers indicate a positive effect and lower numbers indicate a negative effect. The haptic feedback system had a mean SUS score of 76.45 ± 17.10.

Table 4.2: System usability score for different modalities

Modality	Mean	Standard Deviation
Screen-Based	77.71	12.94
3D Display	79.79	11.89
Augmented Reality	61.04	19.23

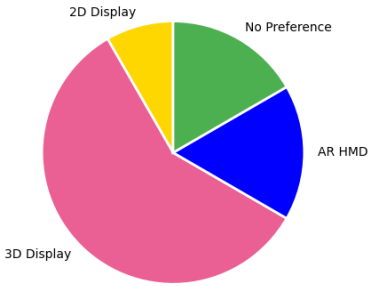

Figure 4.2: Modality preference of users: 2D: 8.333%, 3D: 58.333%, AR HMD: 16.667%, No Preference 16.667%

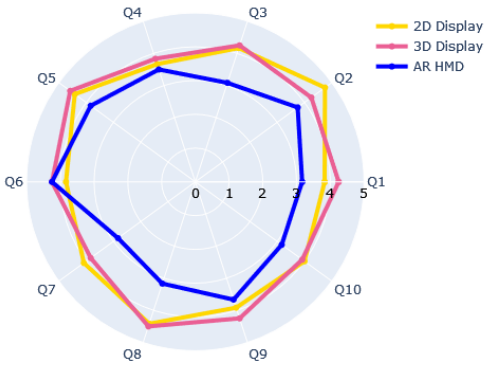

Figure 4.3: Radar chart of the scores on the separate questions. 2D and 3D have relatively similar scores. AR scores remarkably less on Q3, Q7 and Q8

Table 4.3: The SUS questionnaire. 'modality' is replaced by the specific modality in each question.

	Questions
Q1	I think that I would like to use this "modality" system frequently.
Q2	I found the "modality" system unnecessarily complex.
Q3	I thought the "modality" system was easy to use.
Q4	I think that I would need the support of a technical person to be able to use this "modality" system.
Q5	I found the various functions in this "modality" system were well integrated.
Q6	I thought there was too much inconsistency in this "modality" system.
Q7	I would imagine that most people would learn to use this "modality" system very quickly.
Q8	I found the "modality" system very cumbersome to use.
Q9	I felt very confident using the "modality" system
Q10	I needed to learn a lot of things before I could get going with this "modality" system.

5 Discussion

A functional system that is able to perform teleoperated hepatic percutaneous procedures using haptic feedback was realized. The user was able to control a physical needle using a novel haptic AR system. The procedure is visualized using models of the needle and a model of the patient. The system was functional with both a screen setup and the AR HMD. The system met the requirements and could be validated, either by the functioning of the system or the test results. It was found that the most important visual information to show clearly was the pose of the needle, with extra focus on the tip of the needle. Other important visual information were the key points of the operation, the incision point and target point. Further, it was found that the position of visual information in the scene is important, it should not divide the attention of the user and it should not overwhelm them. A comparison was made between different visual modalities, 2D, 3D and AR HMD.

No evidence was found of improved results with AR system compared to both the baseline of a 2D screen and the 3D screen. The AR system scored lower in both usability and accuracy measurements, there is however reduced procedure time compared to 2D. The 2D and 3D display have similar results, with the 3D screen scoring better with procedure time. Most users had a preference for the 3D system. For usability, the 2D and 3D had similar results in all the questions, with only minor differences. The AR system scored noticeably lower in Q3, Q7 and Q8. These mainly relate to the ease of use of the system. This can be explained by limitations in the test setup. 7 of the 12 users wore glasses, which were hard to combine with the magic leap 2. This caused some unconformability with the setup before the experiments even started. Some participants were also not familiar with AR technology at all. Furthermore, with the AR system having a different control scheme, making use of the magic leap controller was somewhat difficult to learn for some of the participants. Finally, the test might have been too limited in what the users had to perform, not showcasing the strengths of the AR system. Since participants could mostly ignore the veins within the procedure. Adding in an extra task such avoiding veins can potentially show the benefits of AR better.

5.1 Limitations

The amount of tests that have been done per participant were limited to prevent them from getting tired and uninterested. Controller of robotic arm is not ideal, a smooth precise immediate motion could not be realized. This was caused by limitations of the MoveIt [46] library. It gave the desired precise movement at the cost of choppy, slow movement. It was opted to use a limited group of 12 students of the UT as participants, these are not the target demographic. The target demographic for the product, if implemented, would be surgeons. The measurement of accuracy was limited by measuring it using the Franka robot. This lacks a secondary measurement for increased accuracy, one that is more linked to the position of the phantom.

6 Conclusion

6.1 Conclusion

A system meeting the requirements was developed. Functioning of the system was showcased with the users, who were able to complete a liver biopsy/ablation procedure on a phantom using a teleoperation setup. Visual guidance was provided using different modalities. AR was incorporated into the system, showing a visual rendering of the teleoperation. The system was capable of performing a hepatic percutaneous teleoperation on a phantom. The performing needle could be controlled using a haptic feedback system. The main benefits of the 3D visualization and AR are reduced procedure time. For AR, these came with the cost of reduced usability. Users gave a preference for use of the 3D display with a wide margin.

6.2 Recommendations and Future work

A different library for the robotic arm control could be selected for future iterations of this project. The MoveIt library[46] is limited in the smoothness of the operation. It could be a major benefit in the performance of the system to develop a better system. Another good addition could be an extension on the haptic feedback system. The current iteration is developed to make movement of the needle in 3D space easy. Further feedback could be added on top of it to provide more control. A haptic feedback device that can incorporate torque feedback could help a lot. The simulation can be made more accurate if the needle position is measured using an additional sensor, preferably one that is viable in vivo teleoperation. This can help demonstrate the viability of the system in vivo teleoperation. For a more accurate representation of AR performance in user testing, individuals with glasses should be excluded. Alternatively, an insert for eyesight can be used or an AR set that is compatible with such individuals.

A Appendix

A.1 Surveys

Below the surveys can be found. The system usability question can be found in table A.1 For the system usability questions the word system was modified to the following words: 3D display system, Augment reality system, screen based system and haptic feedback system. The questions of the pretest survey can found in table A.2. The questions of the post test survey can be found in table A.3.

Table A.1: The questions of the system usability scale.

Question	**Score (1-5)**
1. I think that I would like to use this system frequently.	
2. I found the system unnecessarily complex.	
3. I thought the system was easy to use.	
4. I think that I would need the support of a technical person to be able to use this system.	
5. I found the various functions in this system were well integrated.	
6. I thought there was too much inconsistency in this system.	
7. I would imagine that most people would learn to use this system very quickly.	
8. I found the system very awkward to use.	
9. I felt very confident using the system.	
10. I needed to learn a lot of things before I could get going with this system.	

Table A.2: Pretest survey

Question	**Response**
1. What is your age?	
2. What is your gender? (Options: Male, Female, Non-binary, Prefer not to say)	
3. Do you have experience with force haptic feedback devices? (1-5)	
4. Do you have experience with AR or VR head mounted display? (1-5, never - weekly)	
5. Do you have experience with glassless 3D displays? (1-5, never - weekly)	
6. How would you rate your overall technological competence? (1-5, beginner - expert)	
7. Are you right-handed, left-handed, or ambidextrous?	
8. How is your vision? (nearsighted/farsighted/normal)	
9. Are you color blind? (yes/no)	

Table A.3: Post-survey

Question	**Response**
1. Any suggestions/remarks about each environment independently?	
2. I prefer (Options: Augmented reality, 3D display, Screen, No preference)	
3. If you have a preference, why?	
4. Notes on your general experience	

What is your gender

12 responses

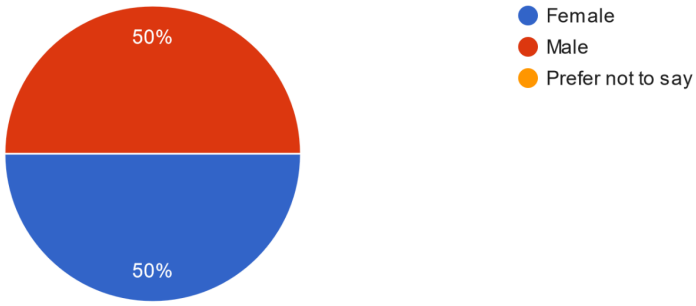

Do you have experience with force haptic feedback devices?

12 responses

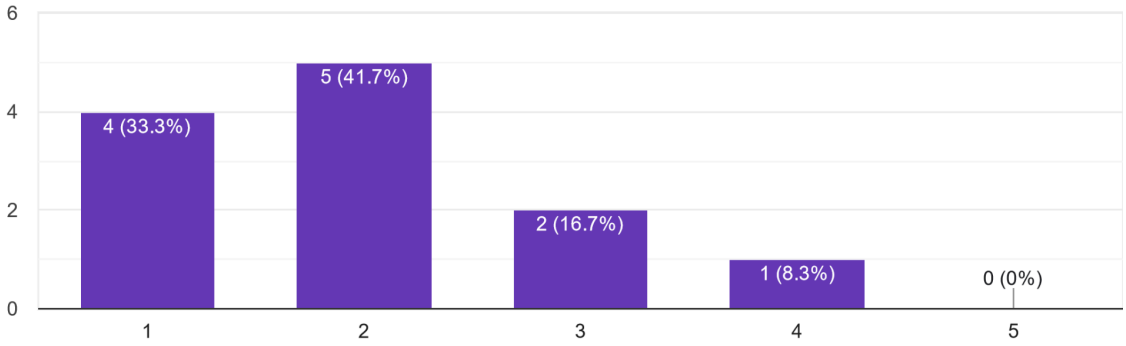

Do you have experience with AR or VR headsets.

12 responses

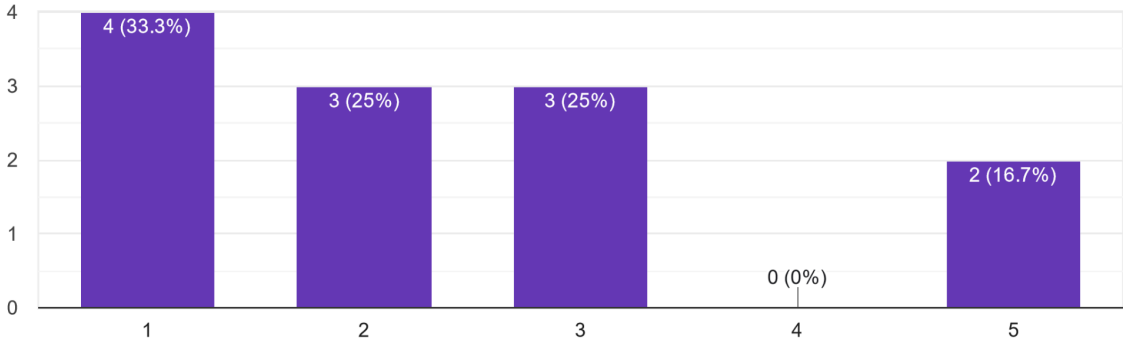

Do you have experience with 3D displays

12 responses

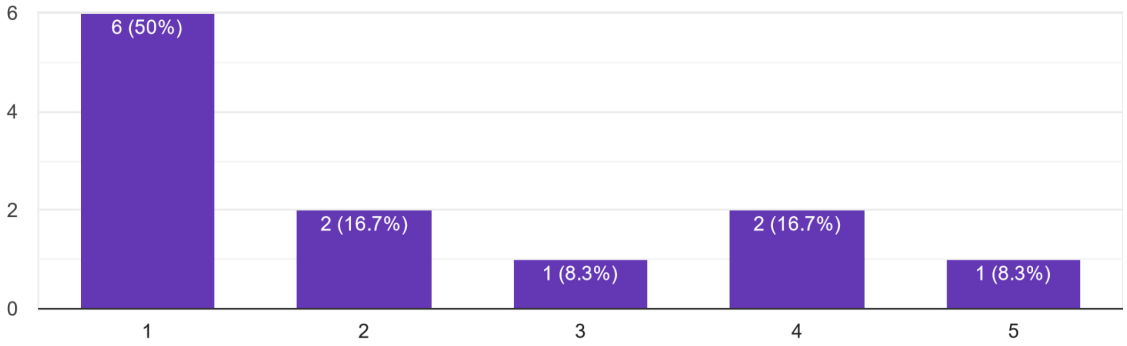

How would you rate your overall technological competence?

12 responses

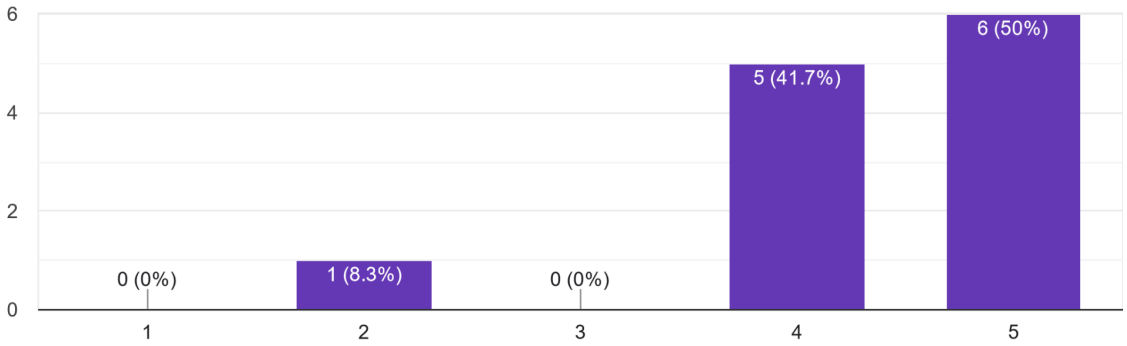

What is your dominant hand?

12 responses

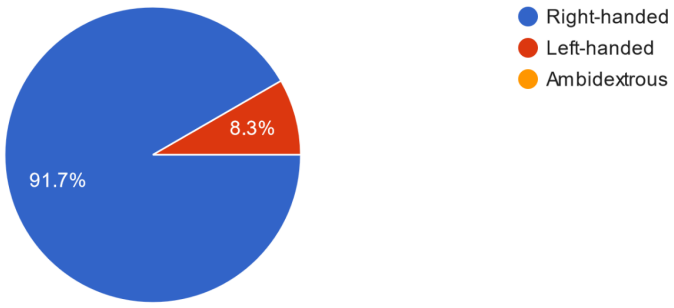

How is your vision?

12 responses

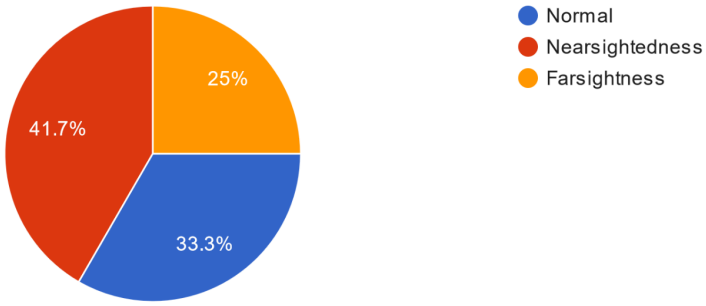

Are you color blind

12 responses

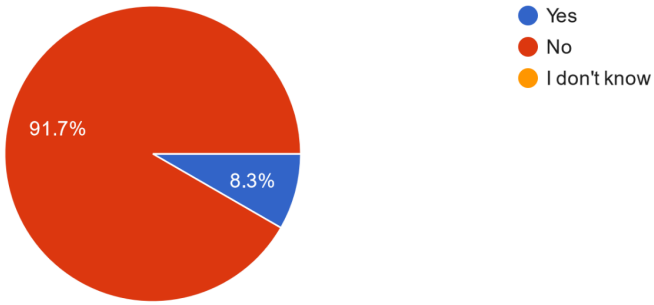

Bibliography

[1] National Cancer Institute. *Liver Cancer Treatment (PDQ) - Patient Version*. Accessed: 2023-11-21.

[2] B. Acidi et al. "Augmented reality in liver surgery". en. In: *Journal of Visceral Surgery* 160.2 (Apr. 2023), pp. 118–126. ISSN: 18787886. DOI: 10.1016/j.jviscsurg.2023.01.008. URL: https://linkinghub.elsevier.com/retrieve/pii/S1878788623000139 (visited on 17/11/2023).

[3] Giuseppe Quero et al. "Virtual and Augmented Reality in Oncologic Liver Surgery". en. In: *Surgical Oncology Clinics of North America* 28.1 (Jan. 2019), pp. 31–44. ISSN: 10553207. DOI: 10.1016/j.soc.2018.08.002. URL: https://linkinghub.elsevier.com/retrieve/pii/S1055320718306835 (visited on 17/11/2023).

[4] Intuitive Surgical, Inc. "da Vinci Surgical System". In: (). Accessed: 2023-11-21.

[5] Benish Fida et al. "Augmented reality in open surgery". en. In: *Updates in Surgery* 70.3 (Sept. 2018), pp. 389–400. ISSN: 2038-131X, 2038-3312. DOI: 10.1007/s13304-018-0567-8. URL: http://link.springer.com/10.1007/s13304-018-0567-8 (visited on 17/11/2023).

[6] Raffaele Vertucci et al. "History of Augmented Reality". en. In: *Springer Handbook of Augmented Reality*. Ed. by Andrew Yeh Ching Nee and Soh Khim Ong. Series Title: Springer Handbooks. Cham: Springer International Publishing, 2023, pp. 35–50. ISBN: 978-3-030-67821-0 978-3-030-67822-7. DOI: 10.1007/978-3-030-67822-7_2. URL: https://link.springer.com/10.1007/978-3-030-67822-7_2 (visited on 24/11/2023).

[7] Alexander Bornik et al. "Computer-aided liver surgery planning: an augmented reality approach". In: ed. by Robert L. Galloway Jr. San Diego, CA, May 2003, p. 395. DOI: 10.1117/12.479743. URL: http://proceedings.spiedigitallibrary.org/proceeding.aspx?doi=10.1117/12.479743 (visited on 17/11/2023).

[8] Dafnis Cain Villagran-Vizcarra et al. "Applications Analyses, Challenges and Development of Augmented Reality in Education, Industry, Marketing, Medicine, and Entertainment". en. In: *Applied Sciences* 13.5 (Feb. 2023), p. 2766. ISSN: 2076-3417. DOI: 10.3390/app13052766. URL: https://www.mdpi.com/2076-3417/13/5/2766 (visited on 17/11/2023).

[9] Anmol Mohan et al. "Telesurgery and Robotics: An Improved and Efficient Era". en. In: *Cureus* (Mar. 2021). ISSN: 2168-8184. DOI: 10.7759/cureus.14124. URL: https://www.cureus.com/articles/54068-telesurgery-and-robotics-an-improved-and-efficient-era (visited on 17/11/2023).

[10] Abrar Gani et al. "Impact of haptic feedback on surgical training outcomes: A Randomised Controlled Trial of haptic versus non-haptic immersive virtual reality training". en. In: *Annals of Medicine & Surgery* 83 (Nov. 2022). ISSN: 2049-0801. DOI: 10.1016/j.amsu.2022.104734. URL: https://journals.lww.com/10.1016/j.amsu.2022.104734 (visited on 01/12/2023).

[11] Yongqing Fu et al. "Robot-Assisted Teleoperation Ultrasound System Based on Fusion of Augmented Reality and Predictive Force". In: *IEEE Transactions on Industrial Electronics* 70.7 (July 2023), pp. 7449–7456. ISSN: 0278-0046, 1557-9948. DOI: 10.1109/TIE.2022.3201322. URL: https://ieeexplore.ieee.org/document/9870621/ (visited on 18/10/2023).

[12] Florian Heinrich et al. “Comparison of Augmented Reality Display Techniques to Support Medical Needle Insertion”. In: *IEEE Transactions on Visualization and Computer Graphics* 26.12 (Dec. 2020), pp. 3568–3575. ISSN: 1077-2626, 1941-0506, 2160-9306. DOI: 10.1109/TVCG.2020.3023637. URL: https://ieeexplore.ieee.org/document/9211732/ (visited on 11/10/2023).

[13] Louis Rosenberg. “The Use of Virtual Fixtures as Perceptual Overlays to Enhance Operator Performance in Remote Environments”. In: (Sept. 1992), p. 52.

[14] Interaction Design Foundation - IxDF. *What is Extended Reality (XR)?* Accessed: Jan. 26, 2024. Publication date not provided.

[15] Andy Wai Kan Yeung et al. “Virtual and Augmented Reality Applications in Medicine: Analysis of the Scientific Literature”. en. In: *Journal of Medical Internet Research* 23.2 (Feb. 2021), e25499. ISSN: 1438-8871. DOI: 10.2196/25499. URL: http://www.jmir.org/2021/2/e25499/ (visited on 26/01/2024).

[16] Marco Solbiati et al. “Thermal Ablation of Liver Tumors Guided by Augmented Reality: An Initial Clinical Experience”. en. In: *Cancers* 14.5 (Mar. 2022), p. 1312. ISSN: 2072-6694. DOI: 10.3390/cancers14051312. URL: https://www.mdpi.com/2072-6694/14/5/1312 (visited on 26/01/2024).

[17] Martin S. Banks et al. “3D Displays”. eng. In: *Annual Review of Vision Science* 2 (Oct. 2016), pp. 397–435. ISSN: 2374-4650. DOI: 10.1146/annurev-vision-082114-035800.

[18] Fuhao Chen, Chengfeng Qiu and Zhaojun Liu. “Investigation of Autostereoscopic Displays Based on Various Display Technologies”. en. In: *Nanomaterials* 12.3 (Jan. 2022), p. 429. ISSN: 2079-4991. DOI: 10.3390/nano12030429. URL: https://www.mdpi.com/2079-4991/12/3/429 (visited on 03/05/2024).

[19] Petr Kellnhofer et al. “Motion parallax in stereo 3D: model and applications”. en. In: *ACM Transactions on Graphics* 35.6 (Nov. 2016), pp. 1–12. ISSN: 0730-0301, 1557-7368. DOI: 10.1145/2980179.2980230. URL: https://dl.acm.org/doi/10.1145/2980179.2980230 (visited on 09/07/2024).

[20] Yanhui Yang and Huang Wu. “Screening for Stereopsis of Children Using an Autostereoscopic Smartphone”. en. In: *Journal of Ophthalmology* 2019 (Oct. 2019), pp. 1–9. ISSN: 2090-004X, 2090-0058. DOI: 10.1155/2019/1570309. URL: https://www.hindawi.com/journals/joph/2019/1570309/ (visited on 17/08/2024).

[21] Muhammad Hammad Malik and Waleed Brinjikji. “Feasibility of telesurgery in the modern era”. en. In: *The Neuroradiology Journal* 35.4 (Aug. 2022), pp. 423–426. ISSN: 1971-4009, 2385-1996. DOI: 10.1177/19714009221083141. URL: http://journals.sagepub.com/doi/10.1177/19714009221083141 (visited on 05/04/2024).

[22] Paul J. Choi, Rod J. Oskouian and R. Shane Tubbs. “Telesurgery: Past, Present, and Future”. eng. In: *Cureus* 10.5 (May 2018), e2716. ISSN: 2168-8184. DOI: 10.7759/cureus.2716.

[23] Sylvia L. Alip et al. “Future Platforms of Robotic Surgery”. en. In: *Urologic Clinics of North America* 49.1 (Feb. 2022), pp. 23–38. ISSN: 00940143. DOI: 10.1016/j.ucl.2021.07.008. URL: https://linkinghub.elsevier.com/retrieve/pii/S0094014321018723 (visited on 02/02/2024).

[24] Bernhard Weber and Clara Eichberger. “The Benefits of Haptic Feedback in Telesurgery and Other Teleoperation Systems: A Meta-Analysis”. en. In: *Universal Access in Human-Computer Interaction. Access to Learning, Health and Well-Being*. Ed. by Margherita Antona and Constantine Stephanidis. Vol. 9177. Series Title: Lecture Notes in Computer Science. Cham: Springer International Publishing, 2015, pp. 394–405. ISBN: 978-3-319-20683-7 978-3-319-20684-4. DOI: 10.1007/978-3-319-20684-4_39. URL: http://link.springer.com/10.1007/978-3-319-20684-4_39 (visited on 12/01/2024).

[25] Reno Rudiman. “Minimally invasive gastrointestinal surgery: From past to the future”. en. In: *Annals of Medicine and Surgery* 71 (Nov. 2021), p. 102922. ISSN: 20490801. DOI: 10.1016/j.amsu.2021.102922. URL: https://linkinghub.elsevier.com/retrieve/pii/S2049080121008724 (visited on 16/08/2024).

[26] Stephanie Prater and Julio O. Zayas. “Percutaneous Radiofrequency Ablation of Liver Tumors”. eng. In: *StatPearls*. Treasure Island (FL): StatPearls Publishing, 2024. URL: http://www.ncbi.nlm.nih.gov/books/NBK557730/ (visited on 16/08/2024).

[27] Shivali Malhotra et al. “Augmented Reality in Surgical Navigation: A Review of Evaluation and Validation Metrics”. en. In: *Applied Sciences* 13.3 (Jan. 2023), p. 1629. ISSN: 2076-3417. DOI: 10.3390/app13031629. URL: https://www.mdpi.com/2076-3417/13/3/1629 (visited on 17/11/2023).

[28] Stephen R. Serge, Jonathan A. Stevens and Latika Eifert. “Make it usable: Highlighting the importance of improving the intuitiveness and usability of a computer-based training simulation”. In: *2015 Winter Simulation Conference (WSC)*. 2015, pp. 1056–1067. DOI: 10.1109/WSC.2015.7408233.

[29] Song Xu et al. “Determination of the latency effects on surgical performance and the acceptable latency levels in telesurgery using the dV-Trainer® simulator”. en. In: *Surgical Endoscopy* 28.9 (Sept. 2014), pp. 2569–2576. ISSN: 0930-2794, 1432-2218. DOI: 10.1007/s00464-014-3504-z. URL: http://link.springer.com/10.1007/s00464-014-3504-z (visited on 17/11/2023).

[30] Vr-Compare. *https://vr-compare.com/ar*. Accessed: 2023-11-24.

[31] Franka Robotics, Inc. *Franka Research 3 Robot System*. Accessed: 2023-11-24.

[32] Martin Gromniak et al. “Needle placement accuracy in CT-guided robotic post mortem biopsy”. en. In: *Current Directions in Biomedical Engineering* 6.1 (Sept. 2020), p. 20200031. ISSN: 2364-5504. DOI: 10.1515/cdbme-2020-0031. URL: https://www.degruyter.com/document/doi/10.1515/cdbme-2020-0031/html (visited on 19/08/2024).

[33] Marco Aggravi et al. “Haptic Teleoperation of Flexible Needles Combining 3D Ultrasound Guidance and Needle Tip Force Feedback”. In: *IEEE Robotics and Automation Letters* 6.3 (July 2021), pp. 4859–4866. ISSN: 2377-3766, 2377-3774. DOI: 10.1109/LRA.2021.3068635. URL: https://ieeexplore.ieee.org/document/9385838/ (visited on 18/08/2024).

[34] Open Source Robotics Foundation. *Robot Operating System (ROS)*. Accessed: 2024-06-24. 2024. URL: https://www.ros.org/.

[35] Tianqi Huang et al. “High-performance autostereoscopic display based on the lenticular tracking method”. en. In: *Optics Express* 27.15 (July 2019), p. 20421. ISSN: 1094-4087. DOI: 10.1364/OE.27.020421. URL: https://opg.optica.org/abstract.cfm?URI=oe-27-15-20421 (visited on 16/08/2024).

[36] Sophie A. Armstrong et al. “Tissue-Mimicking Materials for Ultrasound-Guided Needle Intervention Phantoms: A Comprehensive Review”. en. In: *Ultrasound in Medicine & Biology* 49.1 (Jan. 2023), pp. 18–30. ISSN: 03015629. DOI: 10.1016/j.ultrasmedbio.2022.07.016. URL: https://linkinghub.elsevier.com/retrieve/pii/S0301562922005099 (visited on 20/12/2023).

[37] Dilara J. Long et al. “Comparison of Smartphone Augmented Reality, Smartglasses Augmented Reality, and 3D CBCT-guided Fluoroscopy Navigation for Percutaneous Needle Insertion: A Phantom Study”. en. In: *CardioVascular and Interventional Radiology* 44.5 (May 2021), pp. 774–781. ISSN: 0174-1551, 1432-086X. DOI: 10.1007/s00270-020-02760-7. URL: https://link.springer.com/10.1007/s00270-020-02760-7 (visited on 11/10/2023).

[38] Ali Khalifa, Roula Sasso and Don C. Rockey. “Role of Liver Biopsy in Assessment of Radiologically Identified Liver Masses”. en. In: *Digestive Diseases and Sciences* 67.1 (Jan. 2022), pp. 337–343. ISSN: 0163-2116, 1573-2568. DOI: 10.1007/s10620-021-06822-9. URL: https://link.springer.com/10.1007/s10620-021-06822-9 (visited on 05/01/2024).

[39] Alla Vovk et al. “Simulator Sickness in Augmented Reality Training Using the Microsoft HoloLens”. en. In: *Proceedings of the 2018 CHI Conference on Human Factors in Computing Systems*. Montreal QC Canada: ACM, Apr. 2018, pp. 1–9. ISBN: 978-1-4503-5620-6. DOI: 10.1145/3173574.3173783. URL: https://dl.acm.org/doi/10.1145/3173574.3173783 (visited on 24/06/2024).

[40] Leia Inc. *Leia Display Components - Leia Unity Plugin Guide*. https://support.leiainc.com/developer-docs/unity-sdk/leia-unity-plugin-guide/leia-display-components. Accessed: 2024-07-10. 2024.

[41] Unity Technologies. *Shader Graph*. https://unity.com/shader-graph. Version 12.0.0. 2024.

[42] Force Dimension. *User Manual - Omega.X*. Version 3.14.0. Force Dimension. 2021. URL: https://downloads.forcedimension.com/sdk/doc/fdsdk-3.14.0/user%20manual%20-%20omega.x.pdf.

[43] Sakshi Bramhe and Swanand S Pathak. “Robotic Surgery: A Narrative Review”. en. In: *Cureus* (Sept. 2022). ISSN: 2168-8184. DOI: 10.7759/cureus.29179. URL: https://www.cureus.com/articles/107062-robotic-surgery-a-narrative-review (visited on 08/03/2024).

[44] Lloyd N. Trefethen and David III Bau. *Numerical Linear Algebra*. Society for Industrial and Applied Mathematics, 1997. ISBN: 9780898713619, 0898713617.

[45] Jian S. Dai. “Euler–Rodrigues formula variations, quaternion conjugation and intrinsic connections”. en. In: *Mechanism and Machine Theory* 92 (Oct. 2015), pp. 144–152. ISSN: 0094114X. DOI: 10.1016/j.mechmachtheory.2015.03.004. URL: https://linkinghub.elsevier.com/retrieve/pii/S0094114X15000415 (visited on 28/03/2024).

[46] MoveIt. *The moveit motion planning libary*. Accessed: 2024-04-19.

[47] John Brooke. “SUS: A quick and dirty usability scale”. In: *Usability Eval. Ind.* 189 (Nov. 1995).

[48] Mads Soegaard. “System Usability Scale for Data-Driven UX”. In: *Interaction Design Foundation - IxDF* (21st Nov. 2023). URL: https://www.interaction-design.org/literature/article/system-usability-scale.